



# Diverse and unexpected outcomes from oxidation of the platinum(II) anticancer agent [Pt{(p-BrC<sub>6</sub>F<sub>4</sub>)NCH<sub>2</sub>CH<sub>2</sub>NEt<sub>2</sub>}Cl(py)] by hydrogen peroxide

Ruchika Ojha<sup>a</sup>, Dayna Mason<sup>a</sup>, Craig M. Forsyth<sup>a</sup>, Glen B. Deacon<sup>a,\*</sup>, Peter C. Junk<sup>b,\*</sup>, Alan M. Bond<sup>a,\*</sup>

<sup>a</sup> School of Chemistry, Monash University, Clayton 3800, VIC, Australia

<sup>b</sup> College of Science & Engineering, James Cook University, Townsville, Qld 4811, Australia

## ARTICLE INFO

### Keywords:

Platinum anti-tumour agents  
Oxidation  
Hydrogen peroxide  
Oxidation of the ligand  
Br liberation  
Olefinic substitution

## ABSTRACT

Oxidation of the anti-tumour agent [Pt{(p-BrC<sub>6</sub>F<sub>4</sub>)NCH<sub>2</sub>CH<sub>2</sub>NEt<sub>2</sub>}Cl(py)], **1** (py = pyridine) with hydrogen peroxide under a variety of conditions yields a range of organoamineamidoplatinum(II) compounds [Pt{(p-BrC<sub>6</sub>F<sub>4</sub>)NCH=C(X)NEt<sub>2</sub>}Cl(py)] (X = H, Cl, Br) as well as species with shared occupancy involving H, Cl and Br. Thus, oxidation of the -CH<sub>2</sub>-CH<sub>2</sub>- backbone (dehydrogenation) occurs, often accompanied by substitution. Oxidation of **1** with H<sub>2</sub>O<sub>2</sub> in acetone yielded 1:1 co-crystallized [Pt{(p-BrC<sub>6</sub>F<sub>4</sub>)NCH=CHNEt<sub>2</sub>}Cl(py)], **1H** and [Pt{(p-BrC<sub>6</sub>F<sub>4</sub>)NCH=C(Cl)NEt<sub>2</sub>}Cl(py)], **1Cl**. The former was obtained pure in low yield from the oxidation of **1** with (NH<sub>4</sub>)<sub>2</sub>[Ce(NO<sub>3</sub>)<sub>6</sub>] in acetone, and the latter was obtained from **1** and H<sub>2</sub>O<sub>2</sub> in CH<sub>2</sub>Cl<sub>2</sub> at near reflux. From the latter reaction under vigorous refluxing [Pt{(p-BrC<sub>6</sub>F<sub>4</sub>)NCH=C(Br)NEt<sub>2</sub>}Cl(py)], **1Br** was isolated. In refluxing acetonitrile, oxidation of **1** with H<sub>2</sub>O<sub>2</sub> yielded [Pt{(p-BrC<sub>6</sub>F<sub>4</sub>)NCH=C(H<sub>0.25</sub>Br<sub>0.75</sub>)NEt<sub>2</sub>}Cl(py)], **1H<sub>0.25</sub>Br<sub>0.75</sub>**, in which the alkene is mainly substituted by Br in a dual occupancy. Treatment of **1** with H<sub>2</sub>O<sub>2</sub> and tetrabutylammonium hydroxide in acetone at room temperature formed [Pt{(p-HC<sub>6</sub>F<sub>4</sub>)NCH<sub>2</sub>CH<sub>2</sub>NEt<sub>2</sub>}Cl(py)], **2**. Oxidation of [Pt{(p-HC<sub>6</sub>F<sub>4</sub>)NCH<sub>2</sub>CH<sub>2</sub>NEt<sub>2</sub>}Br(py)], **3** with H<sub>2</sub>O<sub>2</sub> in boiling acetonitrile gave the ligand oxidation product [Pt{(p-HC<sub>6</sub>F<sub>4</sub>)NCH=C(Br)NEt<sub>2</sub>}Br(py)], **3Br**. All major products were identified by X-ray crystallography as well as by <sup>1</sup>H and <sup>19</sup>F NMR spectra. In cases of mixed crystals or dual occupancy compounds, the <sup>19</sup>F and <sup>1</sup>H NMR spectra showed dissociation into the components in the solution in the same proportions as in isolated crystalline material.

## 1. Introduction

Today almost 50% of the cancer patients who receive chemotherapy are treated with platinum anticancer drugs [1]. Despite the success [2–7], clinically used Pt anticancer drugs exhibit intrinsic or acquired resistance [8,9] and side effects such as nephrotoxicity, neurotoxicity and myelosuppression [8–15]. Besides, only 1% of cisplatin forms adducts with DNA after its intravenous administration, while most react with other biomolecules [16]. Eventually, these metal-based anticancer drugs can disturb the cellular redox homeostasis [17,18] and this perturbation is related to side effects like nephrotoxicity and resistance of cisplatin [19,20]. Several reports have investigated the effect of platinum(II) drugs on redox homeostasis of cancer cells [21–25].

Eventually, after intensive research [26–28], the need to reduce side

effects and to expand their usage against a wider range of tumours elaborated the area of research beyond structure-activity rules (SAR) [29]. This broader platform introduced “rule breaker” [30] or “non-traditional” drugs [31] which violate the previously established structure-activity rules [29]. The polynuclear platinum compound BBR3464 is one such compound [32–34]. Amongst the “rule breakers” are two classes of organoamidoplatinum(II) compounds, namely *Class 1*, [Pt{N(R)CH<sub>2</sub>}<sub>2</sub>(py)<sub>2</sub>] (R = polyfluoroaryl) with no H atoms on the N-donor atoms and *Class 2*, *trans*-[Pt{N(R)CH<sub>2</sub>CH<sub>2</sub>NR’<sub>2</sub>}X(py)] (R = polyfluoroaryl; R’ = Et, Me; and X = Cl, Br, I) with *trans* amine ligands and *trans* anionic ligands, and no H atoms on the N-donor atoms (see Fig. 1). Both classes have shown anticancer activity in vitro and in vivo [35,36]. To this stage, *Class 1* has the greater activity, and is more developed. Recently, the leading compound [Pt{(p-HC<sub>6</sub>F<sub>4</sub>)NCH<sub>2</sub>}<sub>2</sub>(py)<sub>2</sub>] (Pt103)

\* Corresponding authors.

E-mail addresses: [glen.deacon@monash.edu](mailto:glen.deacon@monash.edu) (G.B. Deacon), [peter.junk@jcu.edu.au](mailto:peter.junk@jcu.edu.au) (P.C. Junk), [alan.bond@monash.edu](mailto:alan.bond@monash.edu) (A.M. Bond).

<https://doi.org/10.1016/j.jinorgbio.2021.111360>

Received 16 August 2020; Received in revised form 17 January 2021; Accepted 17 January 2021

Available online 5 February 2021

0162-0134/© 2021 Elsevier Inc. All rights reserved.

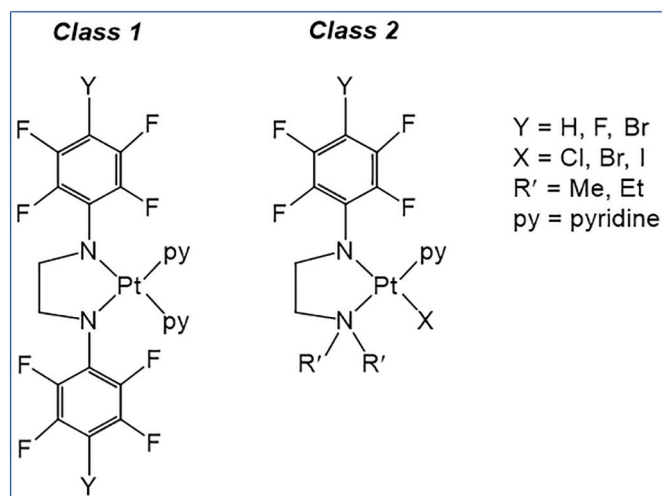


Fig. 1. Class 1 and Class 2 organoamido platinum(II) compounds.

been shown by atomic telemetry and multiscale molecular dynamics to initially bind to adenine rather than guanine, thus explaining some of its unique properties [37]. Binding of the compound to DNA has been detected through attenuated total reflection Fourier transform infrared (ATR-FTIR) spectroscopy [38] and it has been located in a metaphase chromosome by atomic force microscopy-based infrared (AFM-IR) spectroscopy coupled with principal component analysis (PCA) [39]. The leading compound has been converted by photochemical substitution into  $[\text{Pt}\{(p\text{-HC}_6\text{F}_4)\text{NCH}_2\text{CH}_2\text{NH}(p\text{-HC}_6\text{F}_4)\}(\text{py})(\text{O}_2\text{CR})]$ , (R =  $\text{C}_6\text{F}_5$  or 2,4,6- $\text{Me}_3\text{C}_6\text{H}_2$ ) which can be viewed as intermediate between Class 1 and Class 2. These compounds have shown activity against A2780 and A2780/R ovarian cancer cells with the change being detected by ATR-FTIR spectroscopy [40] and the interactions with DNA have also been detected by ATR-FTIR spectroscopy combined with principal component analysis [41].

The redox chemistry of  $\text{Pt}^{\text{II}}$  anticancer compounds is important to comprehend their reactivity in terms of generating  $\text{Pt}^{\text{IV}}$  compounds [42,43]. These are also of biological interest because they are more inert than  $\text{Pt}^{\text{II}}$  species and thus more likely to reach targets without side reactions [49,50] and may be more lipophilic. The chemical oxidation of the Class 1 leading compound  $[\text{Pt}\{(p\text{-HC}_6\text{F}_4)\text{NCH}_2\}_2(\text{py})_2]$ , (Pt103) gave biologically active  $\text{Pt}^{\text{IV}}$  complexes  $[\text{Pt}\{(p\text{-HC}_6\text{F}_4)\text{NCH}_2\}_2(\text{py})_2\text{Cl}_2]$ , (Pt103Cl<sub>2</sub>),  $[\text{Pt}\{(p\text{-HC}_6\text{F}_4)\text{NCH}_2\}_2(\text{py})_2(\text{Cl})\text{OH}]$ , (Pt103(Cl)OH) and  $[\text{Pt}\{(p\text{-HC}_6\text{F}_4)\text{NCH}_2\}_2(\text{py})_2(\text{OH})_2]$ , (Pt103(OH)<sub>2</sub>), all active in vitro. The last two were more active in vivo than the  $\text{Pt}^{\text{II}}$  precursor, Pt103, when delivered in peanut oil [44,45]. The most exciting biological results were obtained for Pt103(OH)<sub>2</sub> which was prepared by oxidation of Pt103 with hydrogen peroxide, thus raising our interest in what might be obtained by oxidation of Class 2 complexes with the same oxidant. Even though hydrogen peroxide is a strong oxidant, it has been extensively used for the oxidation of platinum(II) anticancer agents to less toxic platinum(IV) derivatives [42,44,46–50]. Redox understanding may be relevant to their mode of intracellular action, as in the presence of ROS including  $\text{H}_2\text{O}_2$  in the cell, intracellular oxidation of  $\text{Pt}^{\text{II}}$  compounds may occur [51,52].

We have already examined the electrochemical oxidation of the Class 2 compounds  $\text{trans-}[\text{Pt}\{(p\text{-BrC}_6\text{F}_4)\text{NCH}_2\text{CH}_2\text{NET}_2\}(\text{Cl})(\text{py})]$ , **1** [53] and  $\text{trans-}[\text{Pt}\{(p\text{-HC}_6\text{F}_4)\text{NCH}_2\text{CH}_2\text{NET}_2\}(\text{Cl})(\text{py})]$ , **2** [54] and generated moderately stable formally  $\text{Pt}^{\text{III}}$  monomeric species (formal reversible potentials:  $180 \pm 10$  mV and  $125 \pm 5$  mV vs  $\text{Fc}^{0/+}$  (Fc = Ferrocene) respectively for  $\text{Pt}^{\text{III/III}}$  process), although substantial delocalisation of spin density onto the ligand system is observed [53,54]. Interestingly, no  $\text{Pt}^{\text{IV}}$  species were formed by electrochemical oxidation of this Class in inert dichloromethane media. Because of this and as we were unable to isolate or identify the product of the decay of the formal  $\text{Pt}^{\text{III}}$  species, we

have turned to chemical oxidation to further illuminate the redox properties of the Class 2 compounds.

Here we report the chemical oxidation of the Class 2 complexes  $\text{trans-}[\text{Pt}\{(p\text{-BrC}_6\text{F}_4)\text{NCH}_2\text{CH}_2\text{NET}_2\}(\text{Cl})(\text{py})]$ , **1** (including the formation of  $\text{trans-}[\text{Pt}\{(p\text{-HC}_6\text{F}_4)\text{NCH}_2\text{CH}_2\text{NET}_2\}(\text{Cl})(\text{py})]$ , **2**) and  $\text{trans-}[\text{Pt}\{(p\text{-HC}_6\text{F}_4)\text{NCH}_2\text{CH}_2\text{NET}_2\}(\text{Br})(\text{py})]$ , **3** [55]. These reactions lead to oxidation of the ligand giving organoaminoamido platinum(II) compounds including complexes with substitution of the olefinic moiety, by Cl or Br (Scheme 1) rather than  $\text{Pt}^{\text{IV}}$  derivatives. The antiproliferative activity of **1** in two cell lines was compared with that of  $\text{trans-}[\text{Pt}\{(p\text{-BrC}_6\text{F}_4)\text{NCH}_2\text{CH}_2\text{NET}_2\}(\text{py})]$  **4**.

## 2. Results and discussion

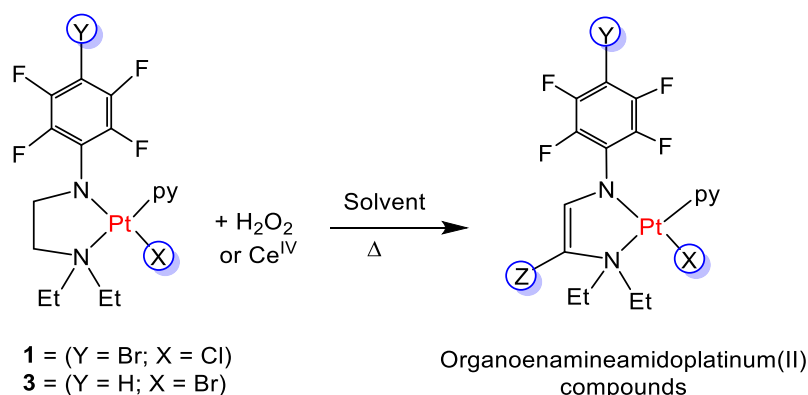
To determine if isolable compounds could be obtained by chemical oxidation of Class 2 compounds, reactions of the organoamido platinum(II) complex  $\text{trans-}[\text{Pt}\{(p\text{-BrC}_6\text{F}_4)\text{NCH}_2\text{CH}_2\text{NET}_2\}(\text{Cl})(\text{py})]$  **1**, were undertaken with hydrogen peroxide at various temperatures and in different solvents. In this case, rather than  $\text{Pt}^{\text{IV}}$  derivatives, organoaminoamido platinum(II) complexes with oxidised ligand e.g., **1H**, **1Cl**, and **1Br** were obtained as shown in Table 1 and Scheme 1 for compound **1**.

The products are  $\text{Pt}^{\text{II}}$  complexes following oxidation of the  $-\text{CH}_2-\text{CH}_2-$  backbone to  $-\text{CH}=\text{CH}-$  and also with halogenation to  $-\text{CH}=\text{CX}-$  (X = Cl or Br). Oxidation involves double ( $\text{sp}^3$ ) C–H bond activation causing dehydrogenation, which then leads to concomitant C=C formation on the backbone of the coordinated ligand. All organoaminoamido platinum(II) complexes discussed have *trans* geometry with the two neutral amine ligands *trans* to each other as are also the two anionic ligands, amide and chloride, as shown in Scheme 1.

The outcome of these oxidation reactions depends on the experimental conditions chosen, as summarized in Scheme 2 and discussed below.

Most reactions gave mixtures of products requiring detailed fractional crystallisation to obtain pure products. In Table 1 are listed the outcomes of oxidation of **1** under a variety of conditions in different solvents. The outcomes were further complicated by co-crystallisation of products and by isolation of products with two substituents disordered at position Z (Scheme 1) on the  $-\text{CH}=\text{C}(\text{Z})-$  backbone. In the cases of mixed occupancies, the ratio of the substituents was established by X-ray crystallography, and dissociation occurred into the individual components in solution in the same ratio as determined by X-ray analysis. Thus **1H**<sub>0.25</sub>**Br**<sub>0.75</sub> in solution gave **1H** and **1Br** in a 1:3 ratio.

A more detailed schematic representation of the oxidation pathways is given in Scheme S1. Prolonged oxidation of **1** with an excess of  $\text{H}_2\text{O}_2$  in warm acetone yields co-crystallised  $\text{trans-}[\text{Pt}\{(p\text{-BrC}_6\text{F}_4)\text{NCH}=\text{CHNET}_2\}(\text{Cl})(\text{py})]$ , **1H** and  $\text{trans-}[\text{Pt}\{(p\text{-BrC}_6\text{F}_4)\text{NCH}=\text{C}(\text{Cl})\text{NET}_2\}(\text{Cl})(\text{py})]$ , **1Cl** (1:1 ratio) in moderate yields on crystallisation from the reaction mixture and also from the crystallisation of additional oily product from acetone/hexane (see experimental). Attempted separation of **1H** and **1Cl** from the oil by chromatography resulted in a few crystals of  $[\text{Pt}\{(p\text{-BrC}_6\text{F}_4)\text{NCH}=\text{CH}_{0.25}\text{Br}_{0.75}\text{NET}_2\}(\text{Cl})(\text{py})]$ , **1H**<sub>0.25</sub>**Br**<sub>0.75</sub>. A pure sample of **1H** was obtained in low yield from the oxidation of **1** with  $(\text{NH}_4)_2[\text{Ce}(\text{NO}_3)_6]$  in acetone. The chlorine substituent of **1Cl** (Z = Cl) at least in acetone, has to be derived from the Pt–Cl bond. Consumption of the complex in supplying Cl or Br limits the possible yields of **1Cl** and **1Br** to  $\leq 50\%$ . From oxidation of **1** with  $\text{H}_2\text{O}_2$  in  $\text{CH}_2\text{Cl}_2$ , pure **1Cl** was obtained in reasonable yield. In the synthesis of **1Cl**, there is a possible alternative source of Cl besides PtCl, namely the solvent. However, a higher  $\text{H}_2\text{O}_2$  to **1** ratio (see entry 2 vs entry 4 in Table 1) with vigorous conditions and longer reaction time did not increase the yield of **1Cl** and instead gave **1Br** in moderate yield (see Scheme 2), hence the solvent is unlikely to be the chloride source. There was the concomitant formation of a trace of  $[\text{Pt}\{(p\text{-BrC}_6\text{F}_4)\text{NCH}=\text{CCl}_{0.5}\text{Br}_{0.5}\text{NET}_2\}(\text{Cl})(\text{py})]$ , **1Cl**<sub>0.5</sub>**Br**<sub>0.5</sub> when a higher  $\text{H}_2\text{O}_2$  to **1** ratio was used with moderate heating. The use of acetonitrile gave a low yield of **1H**<sub>0.25</sub>**Br**<sub>0.75</sub> with some free *pro*-ligand



X	Y	Z	Compounds
Cl	Br	H	<b>1H</b>
Cl	Br	Cl	<b>1Cl</b>
Cl	Br	H <sub>0.25</sub> Br <sub>0.75</sub>	<b>1H<sub>0.25</sub>Br<sub>0.75</sub></b>
Cl	Br	Br	<b>1Br</b>
Cl	Br	Cl <sub>0.5</sub> Br <sub>0.5</sub>	<b>1Cl<sub>0.5</sub>Br<sub>0.5</sub></b>
Br	H	Br	<b>3Br</b>

**Scheme 1.** Oxidation of **1** and **3** with hydrogen peroxide or Ce<sup>IV</sup> give organoeneamineamidoplatinum(II) compounds.

**Table 1**

Quantities of reagents and product yields (crystalline) for the oxidation of **1** and **3** with 30% hydrogen peroxide.

Entry No.	Compound	H <sub>2</sub> O <sub>2</sub> (mmol)	Solvent	Temp and reaction time	Products and yields
1	<b>1</b> (0.20 mmol)	5.00	CH <sub>3</sub> COCH <sub>3</sub>	9 h Δ <sup>a</sup> at 50 °C over 2 d	<b>(1H + 1Cl)</b> <sup>b</sup> = 33%; <b>1H<sub>0.25</sub>Br<sub>0.75</sub></b> = 3%
2	<b>1</b> (0.34 mmol)	8.00	CH <sub>2</sub> Cl <sub>2</sub>	14 h Δ <sup>a</sup> at 25–30 °C over 4 d	<b>1Cl</b> = 39%
3	<b>1</b> (0.20 mmol)	10.0	CH <sub>2</sub> Cl <sub>2</sub>	10 h Δ <sup>a</sup> at 35–40 °C over 3 d	<b>1Br</b> = 31%
4	<b>1</b> (0.20 mmol)	10.0	CH <sub>2</sub> Cl <sub>2</sub>	10 h Δ <sup>a</sup> at 30–35 °C over 2 d	<b>1Cl</b> = 34%; <b>(1Cl<sub>0.5</sub>Br<sub>0.5</sub>)</b> <sup>b, d</sup>
5	<b>1</b> (0.20 mmol)	10.0	CH <sub>3</sub> CN	10 h Δ <sup>a</sup> at 75–82 °C <sup>c</sup> over 2 d	<b>1H<sub>0.25</sub>Br<sub>0.75</sub></b> = 7%; free pro-ligand <sup>d</sup>
6	<b>1</b> (0.50 mmol)	1.00 + 40% NBu <sub>4</sub> OH (1.0 mmol)	CH <sub>3</sub> COCH <sub>3</sub>	4 h Δ <sup>a</sup> at 40–50 °C <sup>c</sup> over 4 d	<b>2</b> = 10%
7	<b>3</b> (0.66 mmol)	10.0	CH <sub>3</sub> CN	7 h Δ <sup>a</sup> at 60 °C <sup>c</sup> over 1 d	<b>3Br</b> = 22%

<sup>a</sup> during the rest of the reaction time (shown in days) the solution was stirred at RT (23 °C).

<sup>b</sup> co-crystallized in 1:1 ratio.

<sup>c</sup> reflux.

<sup>d</sup> yields could not be calculated due to the presence of oily material.

{(p-BrC<sub>6</sub>F<sub>4</sub>)NHCH<sub>2</sub>CH<sub>2</sub>NEt<sub>2</sub>} (see experimental). The crystallisation of the mixed occupancy product is clearly favoured as it has been obtained from two different reactions as shown in [Table 1](#).

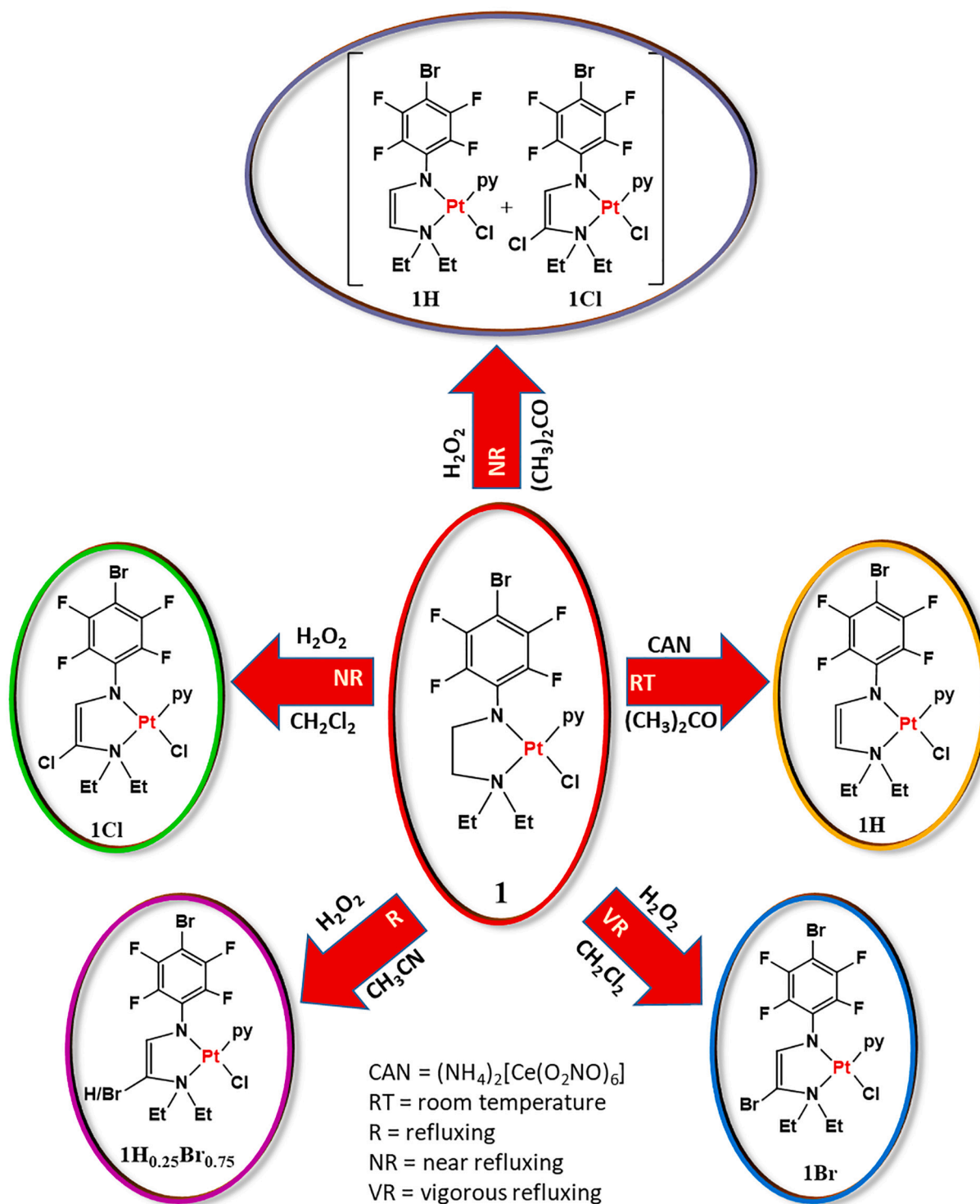
The compounds obtained with Z = Br substituents require Br liberation from the substrate during chemical oxidation with hydrogen peroxide. Evidently, the Br substituent is replaced by an H substituent at the *para* position of the polyfluoroaryl ring, giving *trans*-[Pt{(p-HC<sub>6</sub>F<sub>4</sub>)NCH<sub>2</sub>CH<sub>2</sub>NEt<sub>2</sub>}Cl(py)] **2**. The (p-HC<sub>6</sub>F<sub>4</sub>) resonance can be seen between 5.8 and 6.0 ppm as a multiplet in the <sup>1</sup>H NMR spectrum of crude products when **1Br**, **1H<sub>0.25</sub>Br<sub>0.75</sub>** and **1Cl<sub>0.5</sub>Br<sub>0.5</sub>** are obtained in various reactions ([Fig. S21](#)). Occasionally, a broad resonance at 5.5 ppm was observed in the <sup>1</sup>H NMR spectrum of reaction mixtures after Br liberation, the origin of which could be the presence of an –OH group on the Pt metal center as a replacement for the liberated Cl ligand in [Pt{(p-BrC<sub>6</sub>F<sub>4</sub>)NCH<sub>2</sub>CH<sub>2</sub>NEt<sub>2</sub>}](OH)(py)] (see [Scheme 3](#) and [Fig. S22](#)). Pure *trans*-[Pt{(p-HC<sub>6</sub>F<sub>4</sub>)NCH<sub>2</sub>CH<sub>2</sub>NEt<sub>2</sub>}Cl(py)] (**2**) with the p-H substituent (Y = H) was isolated from the hydrogen peroxide oxidation of **1** in the presence of the base, tetrabutylammonium hydroxide, confirming the lability of the Y = Br substituent.

Oxidation of *trans*-[Pt{(p-HC<sub>6</sub>F<sub>4</sub>)NCH<sub>2</sub>CH<sub>2</sub>NEt<sub>2</sub>}Br(py)], **3** [55] with a 15 fold excess of 30% H<sub>2</sub>O<sub>2</sub> in acetonitrile with heating at 60 °C gave *trans*-[Pt{(p-HC<sub>6</sub>F<sub>4</sub>)NCH=C(Br)NEt<sub>2</sub>}Br(py)], **3Br** ([Table 1](#)) with the Br substituent derived from Pt bound bromo substituent (see [Scheme 3](#)).

The formation of ligand-oxidised Pt<sup>II</sup> species involves double (sp<sup>3</sup>)

C–H bond activation (dehydrogenation) and concomitant C=C formation on the backbone of the coordinated ligand. The oxidation of the –CH<sub>2</sub>–CH<sub>2</sub>– backbone to –CH=CH– by H<sub>2</sub>O<sub>2</sub> is likely to be a radical reaction under the conditions used. Formation of Cl<sub>2</sub> or Br<sub>2</sub> from the oxidation of –Pt–Cl (in **1**) or –Pt–Br (in **3**) bonds and oxidative removal of bromine from the p-BrC<sub>6</sub>F<sub>4</sub> group (i.e., Br liberation from **1**) are considered to be followed by radical halogenation of –CH=CH– to give –CHZ–CHZ– (Z = Cl or Br), which undergoes dehydrohalogenation to the observed –CH=CZ– species. The direction of the elimination suggests a radical process, as a polar dehydrohalogenation might be expected to give an isomer with the halogen adjacent to the fluorocarbon group (cf **1Cl** and **1Br**) owing to the greater acidity of p-BrC<sub>6</sub>F<sub>4</sub>N–CHZ than –CHZNEt<sub>2</sub>.

Unusual transformations of coordinated ligands at transition metal centres have attracted attention in organometallic chemistry due to their use in metal-directed organic synthesis [56,57]. Organozinc-enamines and organoaluminium-enamines with similar oxidised ligands have been reported in the early 1980s where organozinc-enamines were synthesised by the reaction of 1,4-diaza-1,3-butadiene with Et<sub>2</sub>Zn and organoaluminium-enamines were the products of the subsequent transmetalation with Et<sub>3</sub>Al [57,58]. The transformation of the saturated ethylenediamine to dianionic unsaturated diazaethene by dehydrogenation, that is a –CH<sub>2</sub>–CH<sub>2</sub>– backbone to –CH=CH–, has been reported in the reaction of N,N'-diisopropylethylenediamine with a reaction

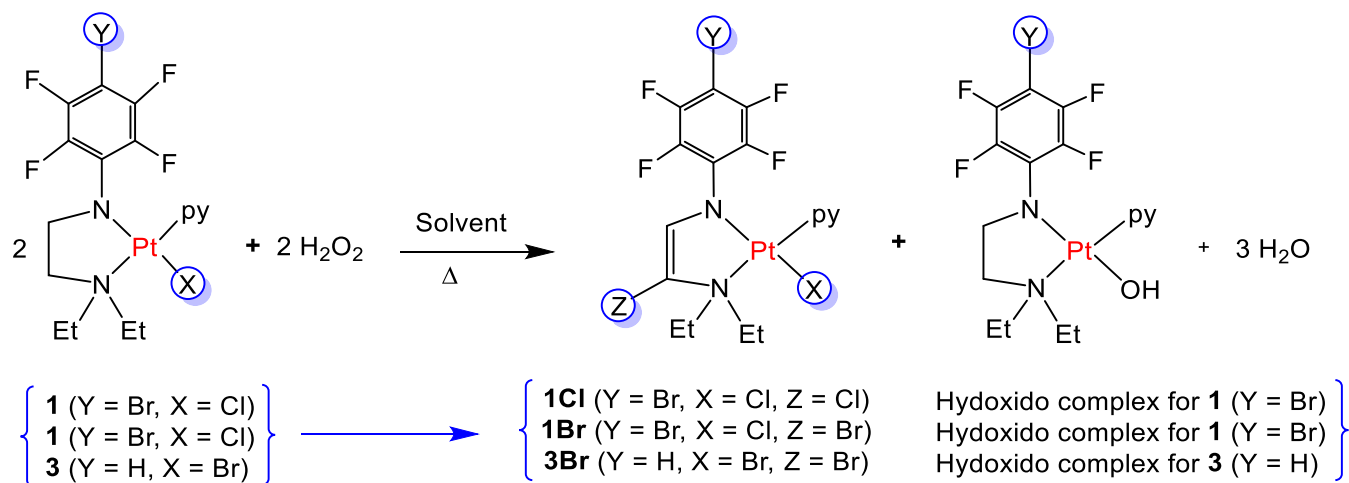
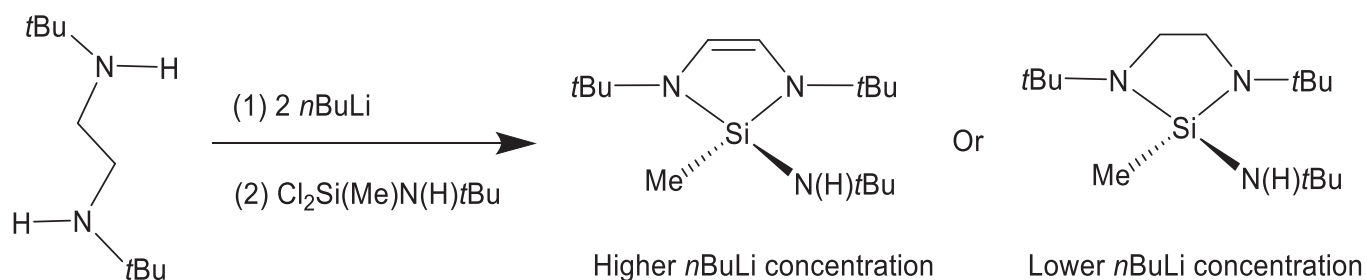
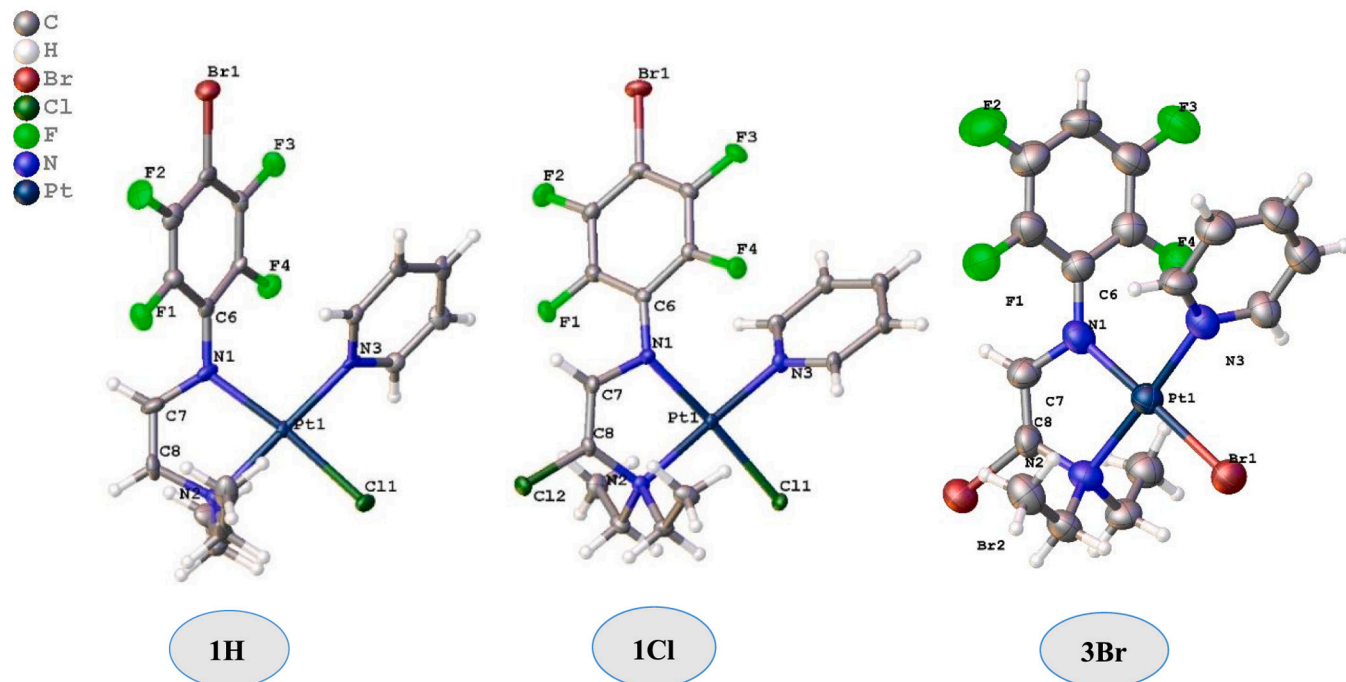


**Scheme 2.** Oxidation of **1** with H<sub>2</sub>O<sub>2</sub> and (NH<sub>4</sub>)<sub>2</sub>[Ce(NO<sub>3</sub>)<sub>6</sub>] under designated conditions. (For interpretation of the references to colour in this figure legend, the reader is referred to the web version of this article.)

mixture containing *n*BuLi and *t*Bu<sub>2</sub>Zn (or Me<sub>2</sub>Zn) [59]. Analogous chelated diamido ligands coordinated to transition metals or lanthanoid metals are also known as catalysts and were obtained from the 1,4-diaza-1,3-diene (DAD) ligand system. For example Veith has reported a dianionic enediamido complex 1,3-diaza-2-silacyclopentene which can only be formed by using a high concentration of *n*BuLi in a reaction with *t*BuN(H)CH<sub>2</sub>CH<sub>2</sub>N(H)*t*Bu and Cl<sub>2</sub>Si(Me)N(H)*t*Bu [60], whereas a lower concentration of *n*BuLi gives [Si{*t*BuNCH<sub>2</sub>CH<sub>2</sub>N*t*Bu}(CH<sub>3</sub>)(N(H)*t*Bu)], the saturated analogue (see Scheme 4) [61].

### 2.1. Characterization

The molecular structures of the products **1H**, **1Cl** and **3Br** isolated from the chemical oxidation reactions of **1** and **3** are shown in Fig. 2 and the crystal structures in Fig. S1. Bond lengths and bond angles of all the oxidised complexes are given in Table 2 and Table S1 respectively. Crystal and refinement data are presented in Table 5. The crystallisation of the organoeneamineidoplatinum complex, *trans*-[Pt{(p-BrC<sub>6</sub>F<sub>4</sub>)NCH=CHNEt<sub>2</sub>}Cl(py)], **1H** is challenging as **1H** can co-crystallise with

Scheme 3. Oxidation of **1** and **3** with an excess of 30% hydrogen peroxide.Scheme 4. Veith's reaction of  $\text{tBuN(H)CH}_2\text{CH}_2\text{N(H)tBu}$  with  $n\text{BuLi}$  and trapping with a dichlorosilane [60,61].Fig. 2. Molecular structures of **1H**, **1Cl**, and **3Br** showing 50% thermal ellipsoids. (For interpretation of the references to colour in this figure legend, the reader is referred to the web version of this article.)

**Table 2**Selected bond lengths for compounds **1H**, **1Cl**, **1H<sub>0.25</sub>Br<sub>0.75</sub>**, **1Cl<sub>0.5</sub>Br<sub>0.5</sub>**, and **3Br**.

Bond	<b>1H</b> (Å) C <sub>17</sub> H <sub>17</sub> BrClF <sub>4</sub> N <sub>3</sub> Pt	<b>1Cl</b> (Å) C <sub>17</sub> H <sub>16</sub> BrCl <sub>2</sub> F <sub>4</sub> N <sub>3</sub> Pt	<b>1H<sub>0.25</sub>Br<sub>0.75</sub></b> (Å) C <sub>17</sub> H <sub>16.25</sub> Br <sub>1.75</sub> ClF <sub>4</sub> N <sub>3</sub> Pt	<b>1Cl<sub>0.5</sub>Br<sub>0.5</sub></b> (Å) C <sub>17</sub> H <sub>16</sub> Br <sub>1.5</sub> Cl <sub>1.5</sub> F <sub>4</sub> N <sub>3</sub> Pt	<b>3Br</b> (Å) C <sub>17</sub> H <sub>17</sub> Br <sub>2</sub> F <sub>4</sub> N <sub>3</sub> Pt
Pt-X	2.325 (5), (X = Cl)	2.3236 (11), (X = Cl)	2.3172 (11), (X = Cl)	2.3107(14), (X = Cl)	2.4404 (10) - 2.4458 (10), (X = Br)
Pt-N1 <sub>(amide)</sub>	2.021 (16)	2.028 (4)	2.022 (4)	2.033 (5)	2.012 (7) - 2.020 (7)
Pt-N2 <sub>(amine)</sub>	2.074 (15)	2.084 (4)	2.085 (4)	2.092 (5)	2.085 (8) - 2.110 (7)
Pt-N3 <sub>(py)</sub>	2.019 (15)	2.013 (4)	2.013 (4)	2.017 (5)	2.003 (7) - 2.023 (8)
N1 <sub>(amide)</sub> -C <sub>6</sub> F <sub>4</sub>	1.40 (2)	1.386 (6)	1.384 (5)	1.376 (7)	1.383 (11) - 1.395 (10)
C7-C8	1.32 (3)	1.337 (7)	1.328 (6)	1.347 (8)	1.321(13) - 1.352 (14)
C8-X	(X = H), 0.950	(X = Cl), 1.764 (5)	(X = Br), 1.854 (4)	(X = Br), 1.871 (6)	(X = Br), 1.895 (9) - 1.916 (9)
N1 <sub>(amide)</sub> -C7	1.35 (3)	1.387 (6)	1.383 (5)	1.379 (7)	1.348 (13) - 1.390 (12)
N2 <sub>(amine)</sub> -C8	1.48 (3)	1.457 (6)	1.454 (6)	1.452 (7)	1.441(12) - 1.448 (12)
N2 <sub>(amine)</sub> -C9 <sub>(Et)</sub>	1.51 (3)	1.511 (6)	1.508 (6)	1.509 (7)	1.505 (13) - 1.519 (11)
N2 <sub>(amine)</sub> -C11 <sub>(Et)</sub>	1.47 (3)	1.518 (6)	1.515 (5)	1.517 (7)	1.441 (12) - 1.535 (11)

\* The asymmetric unit of **3Br** contains 4 molecules, hence the range of the bond lengths for each bond is provided here.

*trans*-[Pt{(p-BrC<sub>6</sub>F<sub>4</sub>)NCH=C(Cl)NEt<sub>2</sub>)Cl(py)], **1Cl** to give **1H** + **1Cl** or have shared occupancy with Br as in **1H<sub>0.25</sub>Br<sub>0.75</sub>** (Fig. S1). However, crystals of pure **1H** were isolated in low yield from the oxidation of **1** (NH<sub>4</sub>)<sub>2</sub>[Ce(NO<sub>3</sub>)<sub>6</sub>] (Fig. 2).

The distinct feature of the organoamineamide complexes is the presence of a double bond which is unsubstituted in **1H** but is substituted by a halogen in **1Cl**, **1Cl<sub>0.5</sub>Br<sub>0.5</sub>**, **1H<sub>0.25</sub>Br<sub>0.75</sub>** and **3Br**, in the NCCN ligand backbone. In all cases, the halogen is located on C8, adjacent to -NEt<sub>2</sub> (Fig. 2 and Fig. S1). In other aspects, these structures are similar to those of the parent reactants **1** [53], and **3** [55]. The C=C bond lengths in the oxidation products are in the range 1.32(3) to 1.347 (8) Å (Table 2). This corresponds to a typical ethene bond length of 1.34 Å [62] and much longer than the C-C backbone in **1** 1.5177(3) Å [53]. In addition the relevant angles around backbone carbons 7 and 8 are ca. 120° (Table S1). Like Class 2 organoamidoplatinum(II) compounds **1–3** [53–55], the organoamineamidoplatinum(II) complexes have square-planar stereochemistry with a *trans* orientation of the donor atoms of like charges e.g., pyridine is *trans* to -NEt<sub>2</sub> and the amido nitrogen is *trans* to the chlorido ligand. The Pt-N2(amine) and Pt-N3(py) bond lengths are similar to those for the parent compounds when 3 esds are taken into account. However, a slight lengthening of the Pt-N1(amide) bond in some cases and a slight shortening of the Pt-Cl bond were observed (see Table 2). The bond angles around the Pt metal are almost 90° and the smallest ≈ 84.08° is affected by the bite angle of the chelating ligand. These bond angles are comparable to those of the parent compound **1** [53] and with **3** [55]. The bond angle sum around the amide N in **1H** (357°), **1Cl** (355.3°) and in **1H<sub>0.25</sub>Br<sub>0.75</sub>** (355.4°), diverge considerably from tetrahedral (∑328.5°) towards triangular (120° ∑360°). The polyfluoroaryl ring is inclined at an angle of 53.60° (**1H**), 55.06° (**1Cl**), 55.49° (**1H<sub>0.25</sub>Br<sub>0.75</sub>**) and 61.14° (**3Br**) to the coordination plane PtN(1)N(2)N(3)Cl, in order to reduce steric hindrance (see Fig. 3), similar to that found with the parent compounds **1** [53] and **3** [55]. This inclined arrangement restricts the delocalisation of the lone pair of the amide N into the polyfluoroaryl ring by resonance, although, considerable inductive delocalisation of electron density is possible due to the presence of electron-withdrawing F atoms in the ring. In almost all the complexes (Fig. 2), the effect of inductive delocalisation is reflected in the bond length of N(amide)-C(C<sub>6</sub>F<sub>4</sub>) ≈ 1.376(7) - 1.40(2) Å (Table 2), which is close to an aromatic bond length [63].

In comparison with Class 2 organoamidoplatinum(II) complexes [53–55], the bond length of N1(amide)-C7, 1.387(6) Å is shorter than a typical C-N bond 1.47 Å (in the parent compound **1** N1-C7 = 1.463 (4) Å) [53] and closer to that of an aromatic bond length. These features imply that a delocalisation across C6N1C7C8 is present in these oxidised Pt<sup>II</sup> complexes. In the case of complexes **1H<sub>0.25</sub>Br<sub>0.75</sub>** and **1Cl<sub>0.5</sub>Br<sub>0.5</sub>**, there is a shared occupancy of substituents attached to C8.

As in the case with parent Class 2 complexes [54], enamineamidoplatinum(II) complexes have a 'W' arrangement of the ethyl groups on the chelating ligand due to agostic interactions. Distances and angles for

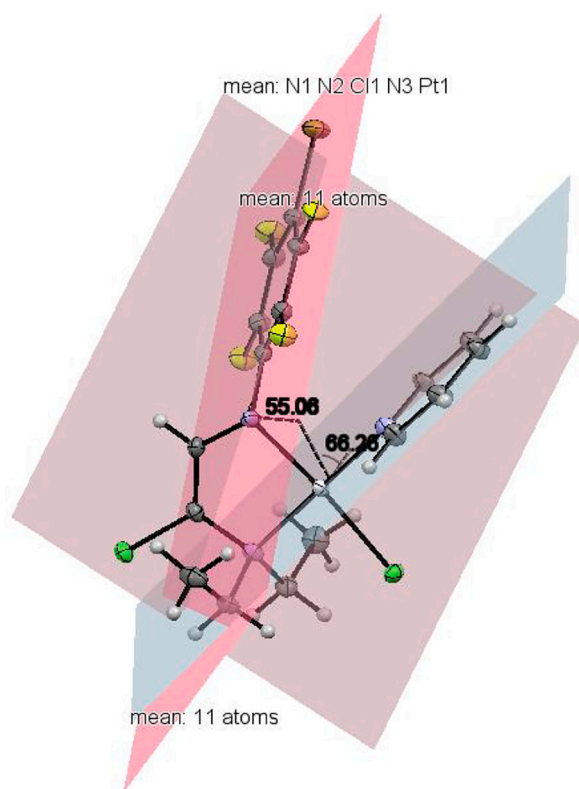


**Fig. 3.** Twisting of the pyridine and polyfluoroaryl ring planes from the coordination plane in **1Cl**. (For interpretation of the references to colour in this figure legend, the reader is referred to the web version of this article.)

agostic interactions for selected compounds are presented in Table S2. The distances are generally within the sum of the Pt and H or C van der Waals radii (2.92 and 3.42 Å, respectively) [64,65].

As observed in Class 2 complexes, a range of supramolecular interactions has been observed in the solid-state of organoamineamidoplatinum(II) complexes. Intermolecular H-bonding forms a 2D sheet and  $\pi$ - $\pi$  interactions between the aromatic rings of these 2D sheets altogether create a 3D network. For example, in **1H**, both *m*-Fs of the polyfluoroaryl ring make H-bonds with F2...*o*-H(py) and F3...H(CH<sub>2</sub>) (2.398(14) Å and 2.448(11) Å respectively) with two other molecules. In addition, *o*-F exhibits H-bonding (F4...*o*-H(py) and F4...*m*-H(py) at 2.654(11) Å and 2.662(12) Å respectively) with one pyridine of another molecule creating a 2D sheet as shown in the Figs. S2-S6. Additional H-bonding such as Br...H(C=C) (3.053(2) Å) and Cl...H(CH<sub>3</sub>) (2.998(5) Å) further supports the structure. Intramolecular H-bonding

between F1...H(CH<sub>3</sub>) with a bond distance of 3.446(12) Å is also observed.

In contrast to **1** [53,66], oxidation and dehydrogenation of the backbone of the coordinated ligand allowed  $\pi$ - $\pi$  interactions for both pyridine and the polyfluoroaryl rings in **1H** in spite of the presence of bulky Br in polyfluoroaryl ring (Fig. S3 and Table S3).  $\pi$ - $\pi$  Interactions between the planes of polyfluoroaryl rings (with inter-planar angle: 0.00°; inter-planar distance: 3.334 Å; inter-centroid distance: 3.809 Å) and between the planes of pyridines (with inter-planar angle: 0.00°; inter-planar distance: 3.278 Å; inter-centroid distance: 3.653 Å) exist which are offset by 1.61 Å for pyridine rings and 1.77 Å for polyfluoroaryl rings (Fig. S3 and Table S3). These  $\pi$ - $\pi$  interactions are further supported by (py) *m*-H...Cl(Pt), 2.871(5) Å for pyridine rings and by various F...H and Br...H interactions for polyfluoroaryl rings as shown in Fig. S3. A discussion of supramolecular interactions in other products is given in the Supporting information.

We have also determined the crystal structure of [Pt{(p-BrC<sub>6</sub>F<sub>4</sub>)NCH<sub>2</sub>CH<sub>2</sub>NEt<sub>2</sub>}I(py)], **4**, which is isostructural with **1**. The crystal structure is shown in Fig. S23 with accompanying bond distances and angles in Table S5. These are as expected with Pt-I bond length 2.6287 (7) Å suitably greater than Pt-Cl 2.3441(10) Å of **1**. However, the crystal packing of **4** is not the same as in **1** and only one of the two ethyl groups shows agostic interaction. A detailed discussion is provided in supporting information (Section 5) and illustrated in Fig. S23.

Satisfactory microanalyses were obtained for all complexes, except for **1H** where the low yield limited identification to NMR spectra and a high-resolution mass spectrum.

All oxidised complexes were characterised by accurate mass protonated molecular ions (M + H)<sup>+</sup>. Interestingly, the protonated molecular ion (M + H)<sup>+</sup> of the starting material (**1**) was not detected under low-resolution mass spectral conditions even though **1** was not detected in <sup>1</sup>H and <sup>19</sup>F NMR spectra. This behaviour suggests that **1** forms under the conditions of obtaining low-resolution mass spectra. However, **1** was not detected in the accurate mass spectra. The difference is attributed to different conditions when determining the different mass spectra (see experimental section).

The most characteristic IR band for enamineamidoplatinum(II) complexes is the stretching (aliphatic) C=C vibration, which is evident in the 1645–1670 cm<sup>-1</sup> region. **1H** shows this C=C stretching band at 1660 cm<sup>-1</sup>, whereas for the halogenated organoamineamide complexes, it appears at 1644–1654 cm<sup>-1</sup>. A comparison of IR data for the Pt<sup>II</sup> precursor **1** and **1H** is provided in Fig. S7. Table 3 summarises C=C stretching data for the complexes with a different substituent at C8, H in **1H**, Cl in **1Cl**, Br in **1Br** and H<sub>0.5</sub>/Cl<sub>0.5</sub> in **1H + 1Cl**. Strong  $\nu$ (C-F) absorption bands appear at comparatively higher wavenumber of 972 cm<sup>-1</sup> (**1H**), 969 cm<sup>-1</sup> (**1Cl**) and 972 cm<sup>-1</sup> (**1H + 1Cl**) than in the platinum(II) precursor **1** at 956 cm<sup>-1</sup>.

The <sup>19</sup>F NMR resonances of the enamineamidoplatinum(II) complexes (**1H-1H<sub>0.25</sub>Br<sub>0.75</sub>**) appear at a higher frequency, (approximately 3 ppm) relative to the parent compound **1**.

Comparison of the <sup>1</sup>H NMR spectrum of **1H** with that of **1** shows two new resonances attributable to HC=CH at around 6.07 (multiplet owing to coupling with ring fluorines in addition to H, H coupling, see Fig. 4) and 3.75 ppm (doublet from coupling with the other alkenyl proton) with large platinum-hydrogen coupling constants, 50 Hz and 34 Hz respectively, and the backbone CH<sub>2</sub> resonances of **1** are absent. These

observations confirm that oxidation of the organoamide ligand has occurred. As pyridine has a greater *trans*-influence than the halide ligands [67,68], the smaller coupling (34 Hz) is expected to be shown by the H attached on the carbon *trans* to pyridine, namely HCNEt<sub>2</sub>, whereas the resonance with a platinum-proton coupling constant of 50 Hz is assigned to HCN(p-BrC<sub>6</sub>F<sub>4</sub>) that is *trans* to chlorine. Also, HCN(p-BrC<sub>6</sub>F<sub>4</sub>) is at a higher frequency than HCNEt<sub>2</sub>, owing to deshielding of the C-H bond of HCN(p-BrC<sub>6</sub>F<sub>4</sub>) by the electron-withdrawing polyfluoroaryl group and the multiplicity of these resonances (see above) also supports these assignments.

In **1Cl**, with a chloro substituted backbone, no HCNEt<sub>2</sub> resonance is observed but the <sup>1</sup>H resonance of HCN(p-BrC<sub>6</sub>F<sub>4</sub>) appears near 6.6 ppm which is at a higher frequency than in **1H** owing to the presence of the adjacent chlorido substituent. This signal at 6.6 ppm appears as two separate triplets with combined integration of one proton and each shows platinum satellites with a platinum-proton coupling constant of 40 Hz (see Fig. 4). The presence of two triplets is unexpected. A two dimensional NMR spectrum showed that these two triplets are associated with two different C atoms in similar environments, hence overall ruling out an assignment as a doublet of triplets. A possible explanation, suggested by a referee, is that the two triplets, of total integration 1H, may arise from the presence of two isomers (termed **I1** and **I2** in the experimental section) owing to interchange of py and Cl ligands in solution. The 1:1 ratio of these is temperature independent (as observed in variable temperature <sup>1</sup>H NMR studies (Fig. S14-S16); the details are provided in the supporting information). Two barely resolved resonances in the <sup>195</sup>Pt NMR spectrum of **1Cl** are consistent with the presence of two similar isomers in solution (Fig. S13).

Notably, the molecular structure of **1Cl** has a delocalised C8C7N1C6 system (Fig. 2 and Table 2) with potential double bond character of the N1 C6 bond. In the parent compound **1**, (p-BrC<sub>6</sub>F<sub>4</sub>)NCH<sub>2</sub> coupling with F of the polyfluoroaryl ring is unresolved but in **1Cl**, due to the presence of a delocalised C8C7N1C6 system, (p-BrC<sub>6</sub>F<sub>4</sub>)NCH, F coupling is resolved. The methylene groups of the -NCH<sub>2</sub>Me in **1H** and **1Cl** give two signals as observed for the parent compound **1** [53] owing to the diastereotopic nature of the methylene protons.

## 2.2. Biological testing

The low yields and difficult syntheses of **1H**, **1Cl** and **1Br** make them unattractive to pursue for biological testing and large scale syntheses would generate considerable toxic waste. However, although a considerable number of *Class 2* compounds have been tested for anti-tumour activity in vitro and some in vivo [36], **1** was not examined. We have now tested this compound together with the iodidoplatinum(II) analogue, [Pt{(p-BrC<sub>6</sub>F<sub>4</sub>)NCH<sub>2</sub>CH<sub>2</sub>NEt<sub>2</sub>}I(py)] **4** against HT-29 colon carcinoma cells and the MCF-7 breast adenocarcinoma cells. The IC<sub>50</sub> values (concentration that causes 50% inhibition of the cell proliferation) for **1** and **4** are summarized in Table 4.

The activity of **1** was comparable with that of cisplatin in both cell lines. However **4** is 7–20 times more active than cisplatin and warrants further examination. The increase in activity is in line with complex stability wherein iodidoplatinum compounds are more stable than chlorido complexes. This trend was noted with other *Class 2* complexes previously though in a different testing regime (L1210 and L1210DDP mouse leukaemia cells) [36]. Thus while the oxidation products are unlikely to be explored further, the parent *Class 2* organoamides still are of interest.

## 3. Conclusion

The generation of organoamineamidoplatinum(II) compounds by chemical oxidation of *trans*-[Pt{(p-BrC<sub>6</sub>F<sub>4</sub>)NCH<sub>2</sub>CH<sub>2</sub>NEt<sub>2</sub>}Cl(py)], **1** and *trans*-[Pt{(p-HC<sub>6</sub>F<sub>4</sub>)NCH<sub>2</sub>CH<sub>2</sub>NEt<sub>2</sub>}Br(py)], **3** with hydrogen peroxide is reported. *Trans*-[Pt{(p-BrC<sub>6</sub>F<sub>4</sub>)NCH=CHNEt<sub>2</sub>}Cl(py)], **1H** was obtained in pure form by oxidation of **1** with ceric ammonium nitrate (CAN,

**Table 3**  
Comparison of C=C stretching (aliphatic) IR vibration data for **1H**, **1Cl**, **1Br** and **1H + 1Cl**.

C-X bond	C=C str (aliphatic) cm <sup>-1</sup>	Compound
HC=C(H)	1660	<b>1H</b>
HC=C(Cl)	1654	<b>1Cl</b>
HC=C(Br)	1645	<b>1Br</b>
HC=C(H <sub>0.5</sub> Cl <sub>0.5</sub> )	1646	<b>1H + 1Cl</b>

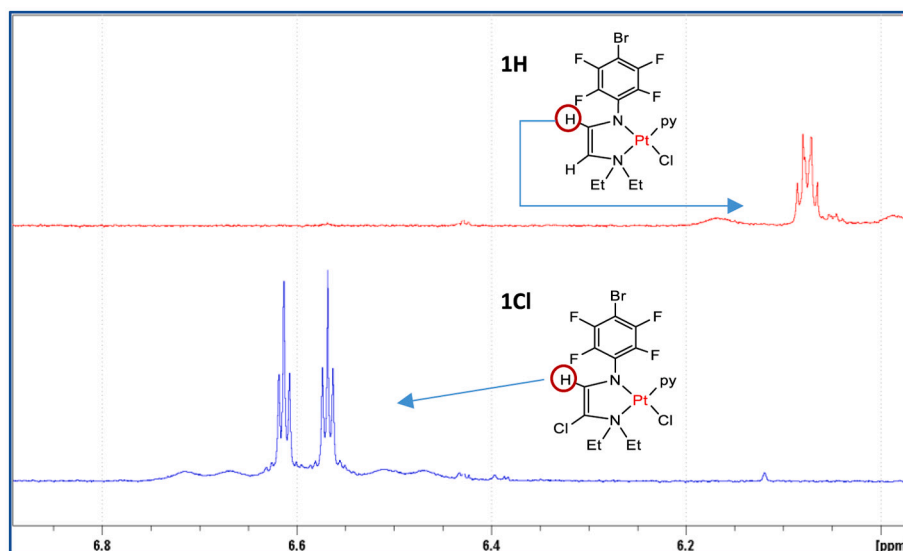


Fig. 4.  $^1\text{H}$  spectra of **1H** (red) and **1Cl** (blue) showing resonances due to  $(p\text{-BrC}_6\text{F}_4)\text{NCH}$ . (For interpretation of the references to colour in this figure legend, the reader is referred to the web version of this article.)

Table 4

IC<sub>50</sub> values obtained from in vitro biological testing of Class 2 organo-amidoplatinum(II) complexes **1** and **4**.

Compound	HT-29* IC <sub>50</sub> [ $\mu\text{M}$ ]	MCF-7# IC <sub>50</sub> [ $\mu\text{M}$ ]
[Pt{(p-BrC <sub>6</sub> F <sub>4</sub> )NCH <sub>2</sub> CH <sub>2</sub> NEt <sub>2</sub> }Cl(py)] <b>1</b>	5.57 ( $\pm 0.45$ )	3.07 ( $\pm 0.55$ )
[Pt{(p-BrC <sub>6</sub> F <sub>4</sub> )NCH <sub>2</sub> CH <sub>2</sub> NEt <sub>2</sub> }I(py)] [ <b>69</b> ]	0.35 ( $\pm 0.12$ )	0.30 ( $\pm 0.03$ )
<b>4</b>		
Cisplatin	7.0	2.0

\* HT-29: Human Colon Carcinoma Cells, (not cisplatin-resistant).

# MCF-7: Human Breast Adenocarcinoma Cells (not cisplatin-resistant).

(NH<sub>4</sub>)<sub>2</sub>[Ce(NO<sub>3</sub>)<sub>6</sub>] but it co-crystallized with *trans*-[Pt{(p-BrC<sub>6</sub>F<sub>4</sub>)NCH=C(Cl)NEt<sub>2</sub>}Cl(py)], **1Cl** in 1:1 ratio when oxidation of **1** was undertaken with H<sub>2</sub>O<sub>2</sub> in acetone. Pure **1Cl** was obtained from **1** and H<sub>2</sub>O<sub>2</sub> in CH<sub>2</sub>Cl<sub>2</sub> at near reflux, whereas vigorous refluxing led to the liberation of the Br substituent from the polyfluoroaryl ring and *trans*-[Pt{(p-

BrC<sub>6</sub>F<sub>4</sub>)NCH=C(Br)NEt<sub>2</sub>}Cl(py)], **1Br** was generated. Overall, this study expands the scope of oxidation of Pt<sup>II</sup> anticancer agents by introducing oxidation of the coordinated ligand. It may provide a tool to modify other platinum(II) anticancer agents to alter their biological activity. It is possible that ligand oxidation is the route by which the formally Pt<sup>III</sup> species generated via electrochemical oxidation of **1** and **2**, decompose. In vitro activity of **1** and **4** against two cell lines shows the former to be comparable with cisplatin, whilst the latter is much more active.

## 4. Experimental

### 4.1. Materials

The following compounds were used as received: acetone (BDH), dichloromethane, acetonitrile (Aldrich), ethyl acetate and *n*-hexane (HPLC grade); hydrogen peroxide (30% solution in water) (Merck) was stored at  $-4^\circ\text{C}$ ; MnO<sub>2</sub>, NBu<sub>4</sub>Cl, LiCl and (NH<sub>4</sub>)<sub>2</sub>[Ce(NO<sub>3</sub>)<sub>6</sub>] (Sigma Aldrich); NBu<sub>4</sub>OH (40% in water) (Fluka).

Table 5

Crystallographic data for the molecular structures of **1H**, **1Cl**, **1H**<sub>0.25</sub>**Br**<sub>0.75</sub>, co-crystallized **1H** + **1Cl**, **1Cl**<sub>0.5</sub>**Br**<sub>0.5</sub> and **3Br**.

	<b>1H</b>	<b>1Cl</b>	<b>1H</b> <sub>0.25</sub> <b>Br</b> <sub>0.75</sub>	<b>1H</b> + <b>1Cl</b>	<b>1Cl</b> <sub>0.5</sub> <b>Br</b> <sub>0.5</sub>	<b>3Br</b>
Empirical formula	C <sub>17</sub> H <sub>17</sub> BrF <sub>4</sub> N <sub>3</sub> PtCl	C <sub>17</sub> H <sub>16</sub> BrF <sub>4</sub> N <sub>3</sub> PtCl <sub>2</sub>	C <sub>17</sub> H <sub>16.25</sub> Br <sub>1.75</sub> ClF <sub>4</sub> N <sub>3</sub> Pt	C <sub>34</sub> H <sub>33</sub> Br <sub>2</sub> Cl <sub>3</sub> F <sub>8</sub> N <sub>6</sub> Pt <sub>2</sub>	C <sub>17</sub> H <sub>16</sub> Br <sub>1.5</sub> Cl <sub>1.5</sub> F <sub>4</sub> N <sub>3</sub> Pt	C <sub>17</sub> H <sub>17</sub> Br <sub>2</sub> F <sub>4</sub> N <sub>3</sub> Pt
Formula weight	649.78	684.22	684.23	1334.01	706.44	694.24
Crystal system	Triclinic	Monoclinic	Monoclinic	Monoclinic	Monoclinic	Triclinic
Space group	P1	P2 <sub>1</sub> /n	P2 <sub>1</sub> /n	P2 <sub>1</sub>	P2 <sub>1</sub> /n	P-1
a (Å)	8.5390 (17)	6.9140 (14)	6.9450 (14)	8.5861 (3)	6.9200 (14)	7.45952 (16)
b (Å)	10.613 (2)	13.607 (3)	13.617 (3)	21.9443 (9)	13.609 (3)	22.3980 (2)
c (Å)	10.846 (2)	21.480 (4)	21.552 (4)	10.5178 (4)	21.496 (4)	24.4897 (2)
$\alpha^\circ$	82.03 (3)	90	90	90	90	84.3586 (8)
$\beta^\circ$	85.47 (3)	94.79 (3)	94.59 (3) <sup>o</sup>	91.856 (2)	94.19 (3)	86.3173 (13)
$\gamma^\circ$	87.28 (3)	90	90	90	90	86.0205 (12)
Vol (Å <sup>3</sup> )	969.7 (3)	2013.7 (7)	2031.6 (7)	1980.68 (13)	2019.0 (7)	4055.25 (10)
Z	2	4	4	2	4	4
$\rho$ (calcd) (g/cm <sup>3</sup> )	2.225	2.2567	2.318	2.237	2.3240	2.274
$\mu$ (mm <sup>-1</sup> )	9.477	9.260	10.523	9.348	10.159	17.962
F(000)	612.0	1282.6	1326.0	1256.0	1317.9	2592.0
Reflections collected/ unique	6,194/3,132	18,512 /5,491	18,811/5,599	11,004/7,239	133,827/4,802	82,783/16,825
R <sub>int</sub>	0.0466	0.0467	0.0598	0.439	0.0508	0.1748
$2\theta_{\text{max}}$ (°)	50	61.4	63.372	52	55.84	153.942
Goodness-of-fit on F <sup>2</sup>	1.176	1.024	1.070	1.080	1.042	1.014
R1 indices [I $\geq 2\sigma$ (I)]	0.0639	0.0383	0.0333	0.0577	0.0358	0.0674
wR2 indices [I $\geq 2\sigma$ (I)]	0.1822	0.0985	0.0840	0.1219	0.0855	0.1671

#### 4.2. Preparation of platinum reagents

Class 2 organoamidoplatinum(II) complexes, *trans*-[Pt{(p-BrC<sub>6</sub>F<sub>4</sub>)NCH<sub>2</sub>CH<sub>2</sub>NEt<sub>2</sub>}Cl(py)] [53] (**1**), *trans*-[Pt{(p-HC<sub>6</sub>F<sub>4</sub>)NCH<sub>2</sub>CH<sub>2</sub>NEt<sub>2</sub>}Br(py)] (**3**) [55] and *trans*-[Pt{(p-BrC<sub>6</sub>F<sub>4</sub>)NCH<sub>2</sub>CH<sub>2</sub>NEt<sub>2</sub>}I(py)] (**4**) [69] were synthesised by using literature methods.

#### 4.3. Instrumentation/analytical procedures

Nuclear magnetic resonance (NMR) spectra were recorded from solutions of deuterated solvents at 27.8 °C (unless otherwise stated) with a Bruker DPX 400 spectrometer supported by Top Spin NMR software on a Windows NT workstation with reference to internal CFCl<sub>3</sub> and tetramethylsilane for <sup>19</sup>F NMR and <sup>1</sup>H NMR spectra respectively. The <sup>195</sup>Pt NMR spectrum was recorded with an Avance Neo 500 NMR spectrometer in (CD<sub>3</sub>)<sub>2</sub>CO at 25 °C with reference to external Na<sub>2</sub>PtCl<sub>6</sub>. 2D NMR spectra (Nuclear Overhauser Effect (NOESY), Correlation Spectroscopy (COSY), and Heteroatom Single Quantum Coherence Spectroscopy (HSQC)) and variable temperature <sup>1</sup>H NMR spectra were recorded with a Bruker 400 spectrometer. Infrared spectra were recorded on a Perkin-Elmer 1600 FT-IR spectrophotometer as Nujol and hexachlorobutadiene (HCB) mulls between NaCl plates or recorded on an Agilent Cary 630 attenuated total reflectance (ATR) spectrometer in the range 4000–600 cm<sup>-1</sup>. Low-resolution electrospray mass spectra were recorded on a Waters micromass ZQ QMS instrument connected to an Agilent 1200 series HPLC system. High-resolution accurate mass measurements were performed on a TOF (Agilent) instrument with a multimode source by using dual method, electrospray ionisation and atmospheric pressure chemical ionisation. Cited *m/z* values for ions of elements with two or more isotopes are the most intense peak of a cluster with the expected isotope pattern. CHN elemental analyses were carried out by the Science Centre, London Metropolitan University Elemental Analyses Service. An electrothermal IA6304 apparatus was used to measure the melting points of the compounds.

#### 4.4. X-ray crystallography

X-ray diffraction data for single crystals of **1H**, **1Cl**, **1H<sub>0.25</sub>Br<sub>0.75</sub>**, and **1Cl<sub>0.5</sub>Br<sub>0.5</sub>** were collected at a wavelength of  $\lambda = 0.71073$  Å using the MX1 beamline at the Australian Synchrotron, Victoria, Australia with Blue Ice [70] graphical user interface (GUI) by using the same method as in the **Experimental** section of a previous report [53]. A single crystal of co-crystallized **1H** + **1Cl** was loaded on to a fine glass fibre or cryoloop using hydrocarbon oil with the temperature kept at 123 K using an open-flow N<sub>2</sub> Oxford Cryosystem. A Bruker Apex II diffractometer was used to collect the data, which was processed using the SAINT [71] program. X-ray diffraction data for the crystals of **3Br** were collected on a Rigaku Synergy S diffractometer with a Cu microsource (CuK $\alpha$  1.54184 Å) and Hipix 6000HE direct photon counting detector and processed using CrysAlisPro v1.171.39.46 (Rigaku OD, Yarnton UK, 2018). Data were processed with the XDS [72] software program. All the structures were solved by using direct methods with SHELXS-97 [73] and refined using conventional alternating least-squares methods with SHELXL-2018 [74]. The program OLEX2 [75] was used as the graphical interface. All non-hydrogen atoms in the structures were refined anisotropically, and hydrogen atoms attached to carbon were placed in calculated positions and allowed to ride on the atom to which they were attached. The low measured diffraction completeness in **1H** is presumably due to hardware constraints (single fixed rotation axis, minimum detector distance) at the MX1 beamline at the Australian Synchrotron. The data for **1H** were twinned and partially modelled as a pseudo merohedral twin in SHELX. In the crystal structure of **1Cl**, the calculated negative residual electron density on Pt01 is presumably an “unresolved absorption artefact”. The X-ray diffraction data for single crystals containing co-crystallized **1H** + **1Cl** have been modelled as a mixture of the two species **1H** and **1Cl** in the non-centrosymmetric space group *P2*<sub>1</sub>. As

such, the model suffers from pseudo symmetry effects which impact upon the anisotropic displacement parameters and the bond distances. Specifically, in the current model, the C–C, C–N and C–F distances of pairs of atoms related by the pseudo-inversion centre have been restrained to be the same. This essentially averages the two unrestrained bond distances and hence improves the standard uncertainties of the values. In particular, the unrestrained C(7)–C(8) and C(27)–C(28) distances were 1.29(3) Å and 1.34(3) Å, respectively. Notably, the four atoms of the ethene backbone are all coplanar (max. Deviation 0.04(1) Å at C(8)), indicative of the presence of a C=C (or a delocalised N-C-C-N) system. The structure also was modelled in the centrosymmetric space group *P2*<sub>1</sub>/*n* as a single molecule with a partially occupied Cl position on the ethene backbone. However, this resulted in a high R-value (>0.15) and very poor refinement characteristics. The bond lengths and angles of co-crystallized **1H** + **1Cl** are similar to those for pure **1H** and **1Cl** given in **Tables 2** and **S2**. In the case of **3Br**, the asymmetric unit contains 4 symmetric non-equivalent molecules with a slight difference in the bond lengths. The crystals of **3Br** were twinned and that could not be resolved.

The crystal data and the crystal structure of **4** are provided in the Supporting information (**Fig. S23**).

Crystallographic data for the structures reported in this paper have been deposited with the Cambridge Crystallographic Data Centre as supplementary number CCDC 2012970 for **1H**, 2012971 for **1Cl**, 2004209 for co-crystallized **1H** + **1Cl**, 2012972 for **1H<sub>0.25</sub>Br<sub>0.75</sub>**, 2012974 for **1Cl<sub>0.5</sub>Br<sub>0.5</sub>**, 2,021,205 for **3Br**, 2021208 for {(p-BrC<sub>6</sub>F<sub>4</sub>)NHCH<sub>2</sub>CH<sub>2</sub>N<sup>+</sup>HEt<sub>2</sub>}Cl<sup>-</sup>, and 2040956 for **4**. Copies of the data can be obtained free of charge at [www.ccdc.cam.ac.uk/data\\_request/cif](http://www.ccdc.cam.ac.uk/data_request/cif).

#### 4.5. Oxidation of **1** by diammonium hexanitratocerate (CAN) - generation of **1H**

A solution of CAN (0.109 g, 0.20 mmol) in 6 ml of acetone was added dropwise to a solution of 0.139 g (0.20 mmol) of **1** in 12 ml of acetone. The reaction mixture was stirred at room temperature for 22 h and was diluted by adding 20 ml of distilled water. No solid was obtained. Hence, the product was extracted with ethyl acetate. All the ethyl acetate extracts were collected and concentrated to 7–9 ml by evaporation and hexane (10 ml) was added until the solution became cloudy. The solution was filtered and then concentrated to 5 ml. Acetone (5 ml) was added and the solution was stored at –10 °C. Yellow crystals were obtained and characterised as **1H** by X-ray crystallography and NMR, IR and mass spectroscopy.

##### [Pt{(p-BrC<sub>6</sub>F<sub>4</sub>)NCH=CHNEt<sub>2</sub>}Cl(py)], **1H**

Metallic yellow coloured blocks. (0.012 g, 12% yield) <sup>19</sup>F NMR ((CD<sub>3</sub>)<sub>2</sub>CO): –148.2 [m, 2 F, F 2,6], –138.2 [m, 2 F, F 3,5]. <sup>1</sup>H NMR ((CD<sub>3</sub>)<sub>2</sub>CO): 1.56 [t, 6H, <sup>3</sup>J<sub>H,H</sub> 7 Hz, NCH<sub>2</sub>CH<sub>3</sub>], 2.30 [m, 2H, NCH<sub>A</sub>H<sub>B</sub>CH<sub>3</sub>], 3.43 [m, 2H, NCH<sub>B</sub>H<sub>A</sub>CH<sub>3</sub>], 3.75 [d, <sup>3</sup>J<sub>H,H</sub> 3.45 Hz, <sup>3</sup>J<sub>H,Pt</sub> 34 Hz, 1H, CHNEt<sub>2</sub>], 6.07 [m with <sup>195</sup>Pt satellites, <sup>3</sup>J<sub>H,Pt</sub> 50 Hz, 1H, CHN (p-BrC<sub>6</sub>F<sub>4</sub>)], 7.19 [m, 2H, **H 3**, **5** (py)], 7.74 [tt, <sup>3</sup>J<sub>H,H</sub> 7.8 Hz, <sup>4</sup>J<sub>H,H</sub> 1 Hz, 1 H, **H 4** (py)], 8.42 [d with <sup>195</sup>Pt satellites, <sup>3</sup>J<sub>H,H</sub> 5.6 Hz, <sup>3</sup>J<sub>H,Pt</sub> 30 Hz, 2H, **H 2**, **6** (py)]. IR: 3058w, 2962w, 2926w, 2868w, 2165w, 2080w, 1660s, 1619s, 1468s, 1451w, 1372 m, 1355 m, 1286w, 1263w, 1224 m, 1190s, 1160w, 1111 m, 1142s, 1087w, 1026 m, 998 m, 972 s, 956 m, 846w, 818 s, 762 s, 741 s, 694 s, 639w, 607 s cm<sup>-1</sup>. ESI *m/z* (+ve): 652.2 (20% (**1** + H)<sup>+</sup>) i.e., (C<sub>17</sub>H<sub>19</sub>BrClF<sub>4</sub>N<sub>3</sub>Pt + H)<sup>+</sup>; acc. Mass/ESI calcd for ((**1H**) + H)<sup>+</sup> i.e., (C<sub>17</sub>H<sub>17</sub>BrClF<sub>4</sub>N<sub>3</sub>Pt{<sup>310</sup>(BrClPt)} + H)<sup>+</sup>: 649.9929, found: 649.9930.

#### 4.6. General method used for oxidation of **1** with hydrogen peroxide

**1** dissolved in the designated solvent was placed in a three-necked round bottom flask fitted with a reflux condenser. Excess 30% hydrogen peroxide was added dropwise and the reaction mixture was stirred at room temperature or occasionally heated in an oil-bath under a light flow of nitrogen gas behind a safety screen as concentrated hydrogen peroxide in the acetone in the presence of acid catalyst can

form the shock and friction sensitive explosive triacetone triperoxide (TATP) [76]. Since the determination of completion of the reaction by TLC was ineffective due to the similarity in retention factors of the products and the starting material, observation of colour-change was used as a method to determine the reaction completion. To catalytically degrade residual hydrogen peroxide, MnO<sub>2</sub> (2–3 g) was added in the cold reaction solution which was stirred for 0.5 h. After filtration through Celite, the reaction solution was concentrated by evaporating carefully to 5–6 ml followed by the addition of water or hexane until the solution turned cloudy. In most cases, a cloudy solution with some oil was obtained which was separated by decanting the cloudy solution. The separated oil was dissolved again in the designated solvent and crystals were then obtained by cooling at –10 °C for 5–6 days. The cloudy solution was concentrated by evaporation and stored at –10 °C. Usually, this fraction gave powder or amorphous flakes which were collected and then recrystallised from appropriate solvent mixtures to obtain crystals suitable for X-ray structural determination. The crystals of all the complexes were washed with hexane.

Variations in the procedures are mentioned below as different solvents, concentration of Class 2 organoamidoplatinum(II) complex, temperature and concentrations of hydrogen peroxide used to optimise the reaction conditions for a specific synthesis. When a mixture of the products was obtained after fractional crystallisation, their ratio as determined by <sup>1</sup>H and <sup>19</sup>F NMR spectroscopy is given in the case of already characterised species. For unidentified products, <sup>1</sup>H and <sup>19</sup>F NMR resonances are given.

#### 4.7. Details of specific conditions used for oxidation of (1) with different amounts of 30% hydrogen peroxide in different solvents

##### 4.7.1. Dichloromethane

###### Method 1

To a solution of **1** (0.224 g, 0.34 mmol) in 20 ml dichloromethane, a 30% solution of H<sub>2</sub>O<sub>2</sub> (0.8 ml, 8.0 mmol, 23 fold excess) was added dropwise and the reaction solution was stirred at room temperature for 1 h under nitrogen. The solution was then heated intermittently at 25–30 °C for 14 h over 4 days under nitrogen. The colour of the solution changed from yellow to deep red after 6 h of heating and then to orange as the reaction progressed. MnO<sub>2</sub> (2 g) was added to degrade the remaining H<sub>2</sub>O<sub>2</sub>. After workup, the solution was concentrated to 5 ml and hexane (6 ml) was added. The solution was stored at –10 °C and bright yellow crystals of **1Cl** were obtained.

[Pt{(p-BrC<sub>6</sub>F<sub>4</sub>)NCH=C(Cl)NEt<sub>2</sub>}Cl(py)] (**1Cl**): Metallic bright yellow coloured blocks. (0.24 g, 39% crystalline yield (crude yield = 47%)). M.P. = 163 °C. <sup>19</sup>F NMR ((CD<sub>3</sub>)<sub>2</sub>CO): –148.0 [m, 2 F, F 2, 6], –137.7 [m, 2 F, F 3,5]. <sup>1</sup>H NMR ((CD<sub>3</sub>)<sub>2</sub>CO): 1.55 [overlapping triplets, 6H, <sup>3</sup>J<sub>H,H</sub> 7 Hz, NCH<sub>2</sub>CH<sub>3</sub> (I1 + I2)], 2.63 [m, 2H, NCH<sub>A</sub>H<sub>B</sub>CH<sub>3</sub>], 3.39 [m, 2H, NCH<sub>B</sub>H<sub>A</sub>CH<sub>3</sub>], 6.57 [t with <sup>195</sup>Pt satellites, <sup>5</sup>J<sub>H,F</sub> 2 Hz, <sup>3</sup>J<sub>H,Pt</sub> 40 Hz, 0.5H, CHN(p-BrC<sub>6</sub>F<sub>4</sub>), I1], 6.61 [t with <sup>195</sup>Pt satellites, <sup>5</sup>J<sub>H,F</sub> 2 Hz, <sup>3</sup>J<sub>H,Pt</sub> 40 Hz, 0.5H, CHN(p-BrC<sub>6</sub>F<sub>4</sub>), I2], 7.07 [m, 2H, H3,5 (py)], 7.61 [tt, <sup>3</sup>J<sub>H,H</sub> 7.7 Hz, J<sub>A,B</sub> 1 Hz, 1H, H4 (py)], 8.38 [d with <sup>195</sup>Pt satellites, <sup>3</sup>J<sub>H,H</sub> 5.6 Hz, <sup>3</sup>J<sub>H,Pt</sub> 35 Hz, 2H, H2,6 (py)]. <sup>195</sup>Pt NMR ((CD<sub>3</sub>)<sub>2</sub>CO): –2226.8 [s, br, 1Pt], –2244.0 [s, br, 1Pt] ppm. IR: 2959w, 2924w, 2874w, 2101w, 2083w, 1979w, 1917w, 1702 m, 1654s, 1611s, 1465s, 1450w, 1376 m, 1312s, 1278w, 1261w, 1210 m, 1139s, 1104s, 1078w, 1018s, 969 s, 872 m, 831 s, 763 s, 738 s, 717w, 689 s cm<sup>–1</sup>. ESI m/z 652.1 (55% (1 + H)<sup>+</sup>) i.e., (C<sub>17</sub>H<sub>19</sub>BrClF<sub>4</sub>N<sub>3</sub>Pt + H<sup>+</sup>); acc. Mass MS/ESI calcd for (1Cl) + H<sup>+</sup> i.e., (C<sub>17</sub>H<sub>16</sub>BrCl<sub>2</sub>F<sub>4</sub>N<sub>3</sub>Pt + H<sup>+</sup>): 683.9536, found: 683.9524. Elemental analysis Calcd for C<sub>17</sub>H<sub>16</sub>BrCl<sub>2</sub>F<sub>4</sub>N<sub>3</sub>Pt<sub>1</sub> (M = 684.28): C, 29.84%; H, 2.36%; N, 6.14%. Found: C, 29.64%; H, 2.52%; N, 5.91%.

###### Method 2

**1** (0.139 g, 0.20 mmol) was dissolved in 20 ml dichloromethane and a 30% solution of H<sub>2</sub>O<sub>2</sub> (1 ml, 10.0 mmol, 50 fold excess) was added dropwise. The solution was heated at near refluxing temperature, 30–35 °C for 10 h over 2 days, during which time the solution changed colour

from the initial yellow to a deep red colour in the first hour and then to bright yellow. MnO<sub>2</sub> (2 g) was then added. Following filtration and evaporation of the solution to 3–4 ml, 5 ml hexane were added. The solution was concentrated by evaporation and stored at –10 °C and bright yellow crystals of **1Cl** were obtained in 34% yield. After collection of these crystals, further evaporation of the mother liquor gave a second crop of **1Cl** and green oil. The green oil was dissolved again in dichloromethane, crystallisation from dichloromethane/hexane produced two crystals of [Pt{(p-BrC<sub>6</sub>F<sub>4</sub>)NCH=C(Cl<sub>0.5</sub>/Br<sub>0.5</sub>)NEt<sub>2</sub>}Cl(py)], **1Cl**<sub>0.5</sub>**Br**<sub>0.5</sub> in 1:1 in a single unit cell (identified by single-crystal X-ray diffraction).

###### Method 3

**1** (0.134 g, 0.2 mmol) was dissolved in 20 ml dichloromethane and a 30% solution of H<sub>2</sub>O<sub>2</sub> (1 ml, 10.0 mmol, 50 fold excess) was added dropwise. Occasionally, the solution was vigorously refluxed for 10 h over 3 days, under nitrogen. The solution changed colour from initial yellow to red in an hour of initial heating and then to very light yellow colour at the end of 3 days when MnO<sub>2</sub> was added. After filtration and evaporation to 3–4 ml, 5 ml hexane was added and the solution was stored at –10 °C for crystallisation. Light yellow crystals of [Pt{(p-BrC<sub>6</sub>F<sub>4</sub>)NCH=C(Br)NEt<sub>2</sub>}Cl(py)], **1Br** (along with some unidentified brown oil) were collected and characterised by <sup>1</sup>H and <sup>19</sup>F NMR spectroscopy, mass spectrometry and elemental analysis.

[Pt{(p-BrC<sub>6</sub>F<sub>4</sub>)NCH=C(Br)NEt<sub>2</sub>}Cl(py)] (**1Br**): Metallic light yellow coloured blocks. (0.05 g, 31% crystalline yield) <sup>19</sup>F NMR ((CD<sub>3</sub>)<sub>2</sub>CO): –148.01 [m, 2 F, F 2, 6], –137.63 [m, 2 F, F 3,5]. <sup>1</sup>H NMR ((CD<sub>3</sub>)<sub>2</sub>CO): 1.55 [overlapping triplets, 6H, <sup>3</sup>J<sub>H,H</sub> 7 Hz, NCH<sub>2</sub>CH<sub>3</sub> (I1 + I2)], 2.65 [m, 2H, NCH<sub>A</sub>H<sub>B</sub>CH<sub>3</sub>], 3.36 [m, 2H, NCH<sub>B</sub>H<sub>A</sub>CH<sub>3</sub>], 6.57 [t with <sup>195</sup>Pt satellites, <sup>5</sup>J<sub>H,F</sub> 2 Hz, <sup>3</sup>J<sub>H,Pt</sub> 40 Hz, 0.5H, CHN(p-BrC<sub>6</sub>F<sub>4</sub>), I1], 6.61 [t with <sup>195</sup>Pt satellites, <sup>5</sup>J<sub>H,F</sub> 2 Hz, <sup>3</sup>J<sub>H,Pt</sub> 40 Hz, 0.5H, CHN(p-BrC<sub>6</sub>F<sub>4</sub>), I2], 7.21 [m, 2H, H3,5 (py)], 7.76 [tt, <sup>3</sup>J<sub>H,H</sub> 7.7 Hz, <sup>4</sup>J<sub>H,H</sub> 1 Hz, 1H, H4 (py)], 8.43 [d with <sup>195</sup>Pt satellites, <sup>3</sup>J<sub>H,H</sub> 5.6 Hz, <sup>3</sup>J<sub>H,Pt</sub> 35 Hz, 2H, H2,6 (py)]. IR: 2959w, 2924w, 2874w, 2058w, 1917w, 1738 m, 1719w, 1702 m, 1645s, 1613s, 1463s, 1451w, 1376 m, 1312s, 1278w, 1261w, 1211 m, 1139s, 1103s, 1079w, 1053s, 1017w, 991 s, 968 s, 906 m, 872 m, 829 s, 763 s, 738 s, 717 s, 688 s, 618 s cm<sup>–1</sup>. acc. Mass MS/ESI calcd for (1Br) + H<sup>+</sup> i.e., (C<sub>17</sub>H<sub>16</sub>Br<sub>2</sub>ClF<sub>4</sub>N<sub>3</sub>Pt + H<sup>+</sup>): 729.9025, found: 729.9020. Elemental analysis Calcd for C<sub>17</sub>H<sub>16</sub>Br<sub>2</sub>ClF<sub>4</sub>N<sub>3</sub>Pt<sub>1.05</sub>CH<sub>2</sub>Cl<sub>2</sub> (M = 771.18): C, 27.26%; H, 2.22%; N, 5.45%. Found: C, 27.05%; H, 2.09%; N, 5.66%.

##### 4.7.2. Acetone

**1** (0.139 g, 0.20 mmol) was dissolved in 20 ml acetone and a 30% H<sub>2</sub>O<sub>2</sub> solution (0.5 ml, 5.0 mmol, 25 fold excess) was added. The reaction mixture was stirred for 2 days with occasional heating for 9 h over 2 days at 50 °C. The solution changed colour from yellow to dark orange and then to bright yellow. MnO<sub>2</sub> (2 g) was added to remove unreacted hydrogen peroxide. After filtration and evaporation of the solution to 3–4 ml, distilled water was added until the solution turned turbid. (a) A very small amount of orange coloured solid obtained by filtration was identified as a mixture of the organoeneamide complexes [Pt{(p-BrC<sub>6</sub>F<sub>4</sub>)NCH=CHNEt<sub>2</sub>}Cl(py)], **1H** and [Pt{(p-BrC<sub>6</sub>F<sub>4</sub>)NCH=C(Cl)NEt<sub>2</sub>}Cl(py)], **1Cl** by NMR only. Slight evaporation of the filtrate gave a dark brown coloured oil which was divided into two parts. (b) The first part was dissolved in acetone and crystallisation from acetone/hexane at –10 °C gave bright yellow crystals which were identified as **1H** + **1Cl** co-crystallized in a 1:1 ratio in the unit cell by single-crystal X-ray diffraction, NMR and mass spectrometry. (c) An attempt was made to isolate **1H** and **1Cl** from the second part of the oil. Column chromatography was used with basic alumina as the stationary phase and ethyl acetate and hexane in 1:1 ratio as the eluent. A yellow band was collected in fractions and slow evaporation gave bright yellow crystals which were identified as [Pt{(p-BrC<sub>6</sub>F<sub>4</sub>)NCH=C(H<sub>0.25</sub>/Br<sub>0.75</sub>)NEt<sub>2</sub>}Cl(py)], **1H**<sub>0.25</sub>**Br**<sub>0.75</sub>. The occupancies of H and Br were determined by X-ray structural determination, however, it dissociates in the solution into **1H** and **1Br** in 1:3 ratio.

(a) Co-crystallized  $[\text{Pt}\{(p\text{-BrC}_6\text{F}_4)\text{NCH}=\text{CHNET}_2\}\text{Cl}(\text{py})] + [\text{Pt}\{(p\text{-BrC}_6\text{F}_4)\text{NCH}=\text{C}(\text{Cl})\text{NET}_2\}\text{Cl}(\text{py})]$ , **1H** + **1Cl** co-crystallized (mole ratio 1:1): Metallic bright yellow coloured blocks. (0.045 g, 33% yield).  $^{19}\text{F}$  NMR ( $\text{CDCl}_3$ ): **1H**: -148.5 [m, 2 F, F 2, 6], -137.6 [m, 2 F, F 3,5]; **1Cl** - 148.3 [m, 2 F, F 2, 6], -136.9 [m, 2 F, F 3,5].  $^1\text{H}$  NMR ( $\text{CDCl}_3$ ): 1.65 [m, 12H,  $^3\text{J}_{\text{H,H}}$  7 Hz,  $\text{NCH}_2\text{CH}_3$ , (**1H** + **1Cl**)], 2.30 [m, 2H,  $\text{NCH}_2\text{CH}_2\text{CH}_3$ , (**1H** + **1Cl**)], 3.43 [m, 2H,  $\text{NCH}_2\text{CH}_2\text{CH}_3$ , (**1H** + **1Cl**)], 3.54 [m, 4H,  $\text{NCH}_2\text{CH}_2\text{CH}_3$ , (**1H** + **1Cl**)], 3.75 [d with  $^{195}\text{Pt}$  satellites,  $^3\text{J}_{\text{H,Pt}}$  3.47 Hz,  $^3\text{J}_{\text{H,Pt}}$  33 Hz, 1H,  $\text{CHNET}_2$ , (**1H**)], 6.07 [m with  $^{195}\text{Pt}$  satellites  $^3\text{J}_{\text{H,Pt}}$  53 Hz, 1H,  $\text{CHN}(p\text{-BrC}_6\text{F}_4)$ , (**1H**)], 6.48 [t with  $^{195}\text{Pt}$  satellites,  $^5\text{J}_{\text{H,F}}$  2 Hz,  $^3\text{J}_{\text{H,Pt}}$  40 Hz, 0.5H,  $\text{CHN}(p\text{-BrC}_6\text{F}_4)$ , (**1Cl**, **1I**)], 6.52 [t with  $^{195}\text{Pt}$  satellites,  $^5\text{J}_{\text{H,F}}$  2 Hz,  $^3\text{J}_{\text{H,Pt}}$  40 Hz, 0.5H,  $\text{CHN}(p\text{-BrC}_6\text{F}_4)$ , (**1Cl**, **1I**)], 7.11 [m, 4H, **H3,5** (py), (**1H** + **1Cl**)], 7.66 [m,  $^3\text{J}_{\text{H,H}}$  7.8 Hz,  $^4\text{J}_{\text{H,H}}$  1 Hz, 2H, **H4** (py), (**1H** + **1Cl**)], 8.50 [t with  $^{195}\text{Pt}$  satellites,  $^3\text{J}_{\text{H,H}}$  6 Hz,  $^3\text{J}_{\text{H,Pt}}$  30 Hz, 4H, **H2,6** (py), (**1H** + **1Cl**)]. IR: 3060w, 2962w, 2926w, 2868w, 2164w, 2050w, 1926w, 1662s, 1646 m, 1619s, 1580 m, 1469s, 1450w, 1372 m, 1355 m, 1288w, 1264w, 1224 m, 1190s, 1143s, 1087w, 1027 m, 972 s, 956 m, 876w, 819 s, 763 s, 741 s, 695 s, 641w, 607 s  $\text{cm}^{-1}$ . ESI  $m/z$  (+ve): 652.2 (20% (**1** +  $\text{H}^+$ )) i.e., ( $\text{C}_{17}\text{H}_{19}\text{BrClF}_4\text{N}_3\text{Pt} + \text{H}^+$ ); acc. Mass MS/ESI calcd for (**1H** +  $\text{H}^+$ ) i.e., ( $\text{C}_{17}\text{H}_{17}\text{BrClF}_4\text{N}_3\text{Pt} + \text{H}^+$ ): 649.9924, found: 649.9930; calcd for (**1Cl** +  $\text{H}^+$ ) i.e., ( $\text{C}_{17}\text{H}_{16}\text{BrCl}_2\text{F}_4\text{N}_3\text{Pt} + \text{H}^+$ ): 683.9536, found: 683.9545.

(b)  $[\text{Pt}\{(p\text{-BrC}_6\text{F}_4)\text{NCH}=\text{C}(\text{H}_{0.25}\text{Br}_{0.75})\text{NET}_2\}\text{Cl}(\text{py})]$ , (**1H<sub>0.25</sub>Br<sub>0.75</sub>**): Metallic yellow coloured triangles. (0.027 g, 7% yield). Elemental analysis Calcd for  $\text{C}_{17}\text{H}_{16.25}\text{Br}_{1.75}\text{Cl}_1\text{F}_4\text{N}_3\text{Pt}_1$  ( $M = 728.68$ ): C, 28.80%; H, 2.31%; N, 5.92%. Found: C, 28.15%; H, 2.25%; N, 5.81%. Acc. Mass MS/ESI calcd for (**1Br** +  $\text{H}^+$ ) i.e., ( $\text{C}_{17}\text{H}_{16}\text{Br}_2\text{ClF}_4\text{N}_3\text{Pt} + \text{H}^+$ ): 729.9025, found: 729.9020, calcd for (**1H** +  $\text{H}^+$ ) i.e., ( $\text{C}_{17}\text{H}_{17}\text{BrClF}_4\text{N}_3\text{Pt} + \text{H}^+$ ): 649.9929, found: 649.9911.

All of the analytically pure sample of **1H<sub>0.25</sub>Br<sub>0.75</sub>** was used for microanalyses and MS measurements. The sample used for the NMR spectra retained some ethyl acetate from the isolation procedure, but indicated clear dissociation into a 1:3 ratio of **1H**:**1Br** (see Supporting Information).

#### 4.7.3. Acetonitrile

A solution of **1** (0.139 g, 0.20 mmol) in 20 ml acetonitrile was treated with 30% solution of  $\text{H}_2\text{O}_2$  (1 ml, 10.0 mmol, 50 fold excess) and the reaction mixture was heated at refluxing temperature 75–80 °C for 10 h over 2 days. The colour of the solution changed from yellow, to red and then bright yellow and  $\text{MnO}_2$  (2 g) was added. After filtration and evaporation to 3–4 ml, distilled water (5–6 ml) was added and the solution turned a little cloudy with no oil formed this time. After concentrating the cloudy solution by slight evaporation, it was stored at -10 °C. Bright yellow crystals of  $[\text{Pt}\{(p\text{-BrC}_6\text{F}_4)\text{NCH}=\text{C}(\text{H}_{0.25}\text{Br}_{0.75})\text{NET}_2\}\text{Cl}(\text{py})]$ , **1H<sub>0.25</sub>Br<sub>0.75</sub>** (0.01 g, 7%) were obtained and identified with X-ray crystallography. An attempt was made to isolate the product from the filtrate with ethyl acetate and it gave 2–3 crystals of **1H<sub>0.25</sub>Br<sub>0.75</sub>** along with a small amount of oily free ligand. **Free pro-ligand**  $^{19}\text{F}$  NMR ( $\text{CD}_3\text{CN}$ ) -136.8 [m, 2 F, F 3,5] -160.1 [m, 2 F, F 2,6].

(See below for details of synthesis and characterisation of the free pro-ligand; the crystal structure of  $\{(p\text{-BrC}_6\text{F}_4)\text{NHCH}_2\text{CH}_2\text{N}^+\text{HEt}_2\}\text{Cl}^-$  salt, crystal data, bond lengths and bond angles are provided in **Fig. S24** and **Table S6**).

#### 4.7.4. Acetone: with added tetrabutylammonium hydroxide ( $\text{NBu}_4\text{OH}$ )

A stoichiometric amount of a 30% solution of hydrogen peroxide (0.1 ml, 1.0 mmol) was added to a solution of **1** (0.325 g, 0.50 mmol) in acetone, followed by addition of a 40% solution of tetrabutylammonium hydroxide (0.65 ml, 1.0 mmol). The reaction mixture was stirred for 7 days in the dark under a low stream of nitrogen, during which time the

solution changed colour from yellow to red. The reaction mixture was then heated to 40–50 °C for 4 h and stirred at room temperature for 4 d, however, the colour of the solution remained red. The reaction mixture was heated again at 40 °C for 9 h and then stirred at room temperature for 2 d.  $\text{MnO}_2$  was added to the resulting orange-red solution and stirred for 0.5 h. The solution was filtered through Celite and the solvent was evaporated to 3 ml. Hexane (2 ml) was added and the reaction mixture was stored at -10 °C. An orange-red coloured oil formed, and bright gold flakes of  $[\text{Pt}\{(p\text{-HC}_6\text{F}_4)\text{NCH}_2\text{CH}_2\text{NET}_2\}\text{Cl}(\text{py})]$ , **2** were obtained.

**Gold flakes, (2):**  $[\text{Pt}\{(p\text{-HC}_6\text{F}_4)\text{NCH}_2\text{CH}_2\text{NET}_2\}\text{Cl}(\text{py})]$ , Bright gold flakes (0.02 g, 10%).  $m/z$  ESI $^+$ : 574.0 (100% ( $[\text{Pt}\{(p\text{-HC}_6\text{F}_4)\text{NCH}_2\text{CH}_2\text{NET}_2\}\text{Cl}(\text{py})] + \text{H}^+$ ), 537.0 (12% ( $[\text{Pt}\{(p\text{-HC}_6\text{F}_4)\text{NCH}_2\text{CH}_2\text{NET}_2\}\text{Cl}(\text{py})] - \text{Cl}^+$ ). Elemental analysis Calcd for  $\text{C}_{17}\text{H}_{20}\text{Cl}_1\text{F}_4\text{N}_3\text{Pt}_1$  ( $M = 572.9$ ): C, 35.64%; H, 3.52%; N, 7.33%. Found: C, 35.72%; H, 3.47%; N, 7.28%. The  $^{19}\text{F}$  and  $^1\text{H}$  NMR and IR data (supporting information) were in agreement with those recently reported [54].

#### 4.8. Oxidation of $[\text{Pt}\{(p\text{-HC}_6\text{F}_4)\text{NCH}_2\text{CH}_2\text{NET}_2\}\text{Br}(\text{py})]$ , **3** with 30% hydrogen peroxide

$[\text{Pt}\{(p\text{-HC}_6\text{F}_4)\text{NCH}_2\text{CH}_2\text{NET}_2\}\text{Br}(\text{py})]$ , (0.41 g, 0.66 mmol) was dissolved in 10 ml acetonitrile and 30% solution of  $\text{H}_2\text{O}_2$  (1 ml, 10.0 mmol) was added dropwise. The solution was heated at 60 °C for 7 h and then stirred for 15 h, during which time the solution changed colour from the initial yellow to deep red colour and then to orange.  $\text{MnO}_2$  (2 g) was then added. Following filtration and evaporation to dryness, the residue was dissolved in 2 ml of acetone and 2 ml hexane was added. The solution was stored at -10 °C and orange crystals of  $[\text{Pt}\{(p\text{-HC}_6\text{F}_4)\text{NCH}=\text{C}(\text{Br})\text{NET}_2\}\text{Br}(\text{py})]$  were obtained.

$[\text{Pt}\{(p\text{-HC}_6\text{F}_4)\text{NCH}=\text{C}(\text{Br})\text{NET}_2\}\text{Br}(\text{py})]$ , **3Br** Orange coloured needles. (0.1018 g, 22% crystalline yield. M.P. = 137 °C.  $^{19}\text{F}$  NMR ( $(\text{CD}_3)_2\text{CO}$ ): -149.3 [m, 2 F, F 2, 6], -142.1 [m, 2 F, F 3,5].  $^1\text{H}$  NMR ( $(\text{CD}_3)_2\text{CO}$ ): 1.69 [t, 6H,  $^3\text{J}_{\text{H,H}}$  6 Hz,  $\text{NCH}_2\text{CH}_3$ ], 2.70 [m, 2H,  $\text{NCH}_2\text{CH}_2\text{CH}_3$ ], 3.60 [m, 2H,  $\text{NCH}_2\text{CH}_2\text{CH}_3$ ], 6.69 [t with  $^{195}\text{Pt}$  satellites,  $^3\text{J}_{\text{H,H}}$  3 Hz,  $^3\text{J}_{\text{H,Pt}}$  40 Hz, 1H, 6.93 [tt,  $^3\text{J}_{\text{H,F}}$  10 Hz,  $^4\text{J}_{\text{H,F}}$  7 Hz, 1H,  $p\text{-HC}_6\text{F}_4$ , 7.30 [t,  $^3\text{J}_{\text{H,H}}$  2Hz 2H, **H3,5** (py)], 7.87 [m, 1H, **H4** (py)], 8.58 [d with  $^{195}\text{Pt}$  satellites,  $^3\text{J}_{\text{H,H}}$  5 Hz,  $^3\text{J}_{\text{H,Pt}}$  40 Hz, 2H, **H2,6** (py)]. IR: 1624s, 1608 m, 1500 vs, 1475 m, 1452s, 13,765 m, 1316s, 1277w, 1225vs, 1173s, 1168s, 1142s, 1100s, 1076w, 1020s, 966 s, 934vs, 880w, 837 m, 818 m, 779w, 763 s, 726 m, 712 m, 690 s, 672w, 662w, 638w  $\text{cm}^{-1}$ . ESMS: 696 (100%) ( $M + \text{H}^+$ ) = ( $\text{C}_{17}\text{H}_{18}\text{Br}_2\text{F}_4\text{N}_3\text{Pt}_1 + \text{H}^+$ ). Elemental analysis Calcd for  $\text{C}_{17}\text{H}_{17}\text{Br}_2\text{F}_4\text{N}_3\text{Pt}_1$  ( $M = 694.22$ ): C, 29.76%; H, 2.51%; N, 6.12%. Found: C, 29.41%; H, 2.47%; N, 6.05%.

#### 4.9. Synthesis of pro-ligand $\{(p\text{-BrC}_6\text{F}_4)\text{NHCH}_2\text{CH}_2\text{NET}_2\}$

Bromopentafluorobenzene (125 mmol) and  $\text{N,N}$ -diethylethane-1,2-diamine (250 mmol) in ethanol (20 ml) were refluxed under nitrogen for 18 h. The solution was evaporated under the reduced pressure and an orange coloured frothy gel was obtained which was shaken with ether/water in a separating funnel. The ether layer was collected and added to a further 3 ether extractions from the aqueous layer. All the combined four extractions were dried over  $\text{MgSO}_4$  for 3 d and then evaporated under the reduced pressure leaving a high boiling point liquid. During the distillation, while heating, the liquid turned dark brown. Double distillation under reduced pressure removed the colour of the liquid largely and a very light yellow coloured liquid was obtained. In this liquid some impurities of the other isomers were observed hence, it was distilled again under reduced pressure but this method did not produce high purity product, hence it was purified by column chromatography. Silica gel was used as stationary phase and the solvent was chloroform. After the evaporation of chloroform pure ligand was obtained in the

form of a colourless high boiling point liquid.

(a)  $\{(p\text{-BrC}_6\text{F}_4)\text{NHCH}_2\text{CH}_2\text{N}^+\text{HEt}_2\}$  Colourless oil. B.p. 98 °C/5 × 10<sup>-2</sup> mmHg. <sup>19</sup>F NMR ((CDCl<sub>3</sub>): -159.2 [d, 2F, F<sub>2,6</sub>], -137.3 [d, 2F, F<sub>3,5</sub>]. <sup>1</sup>H NMR (CDCl<sub>3</sub>): 0.93 [t, <sup>3</sup>J<sub>H,H</sub> 7 Hz, 6H, NCH<sub>2</sub>CH<sub>3</sub>], 2.45 [q, <sup>3</sup>J<sub>H,H</sub> 7 Hz, 4H, NCH<sub>2</sub>CH<sub>3</sub>], 2.56 [t, 2H, <sup>3</sup>J<sub>H,H</sub> 6 Hz, CH<sub>2</sub>NEt<sub>2</sub>], 3.30 [m, 2H, CH<sub>2</sub>N(p-BrC<sub>6</sub>F<sub>4</sub>)], 4.82 [br, 1H, NH]. *m/z* ES<sup>+</sup>: 343.1(100% (M + H)<sup>+</sup>); acc. Mass MS/ESI calcd for (C<sub>12</sub>H<sub>15</sub>F<sub>4</sub>N<sub>2</sub>Br + H<sup>+</sup>): 343.0427, found: 343.0424.

After column chromatography, some off-white/cream coloured crystals of  $\{(p\text{-BrC}_6\text{F}_4)\text{NHCH}_2\text{CH}_2\text{N}^+\text{HEt}_2\}\text{Cl}^-$  were obtained from the chloroform solution of oily ligand on slow evaporation of the solvent and identified by X-ray crystallography as shown in Fig. S24.

(b)  $\{(p\text{-BrC}_6\text{F}_4)\text{NHCH}_2\text{CH}_2\text{N}^+\text{HEt}_2\}\text{Cl}^-$  Colourless crystals <sup>19</sup>F NMR ((CDCl<sub>3</sub>): -158.5 [d, 2F, F<sub>2,6</sub>], -137.05 [d, 2F, F<sub>3,5</sub>]. <sup>1</sup>H NMR (CDCl<sub>3</sub>): 1.11 [t, <sup>3</sup>J<sub>H,H</sub> 7 Hz, 6H, NCH<sub>2</sub>CH<sub>3</sub>], 2.69 [q, <sup>3</sup>J<sub>H,H</sub> 7 Hz, 4H, NCH<sub>2</sub>CH<sub>3</sub>], 2.78 [t, 2H, <sup>3</sup>J<sub>H,H</sub> 6 Hz, CH<sub>2</sub>NEt<sub>2</sub>], 3.50 [m, 2H, CH<sub>2</sub>N(p-BrC<sub>6</sub>F<sub>4</sub>)], 5.128 [br, 1H, NH].

#### 4.10. Biological testing

The cell culture of HT-29 colon carcinoma cells and MCF-7 breast carcinoma cells were performed according to the recently used method [77]. The determination of the antiproliferative effects of compounds 1 and 4 were undertaken by using the same method reported recently [77].

#### Conflict of interest

Authors declare no conflict of interest.

#### Acknowledgements

This paper is dedicated to Prof. Wolfgang Kaim on the occasion of his 70th birthday. AMB gratefully acknowledges financial support from the Australian Research Council (grant DP120101470). RO thanks the Australian Government for the provision of an Australian Postgraduate Award. We are thankful to Assoc. Prof. Kellie Tuck for valuable discussions and Dr. Alasdair McKay for recording the <sup>195</sup>Pt NMR spectrum at the CSIRO laboratories. We extend our gratitude to Prof. Ingo Ott and Julia Schur for conducting biological testing of the compounds at the Technical University of Braunschweig, Germany. X-ray crystallography data collection in this research was undertaken on the MX1 beamline at the Australian Synchrotron, which is a part of ANSTO.[78]

#### Electronic Supplementary Material

Supplementary data to this article can be found online at <https://doi.org/10.1016/j.jinorgbio.2021.111360>.

#### References

- [1] T.C. Johnstone, G.Y. Park, S.J. Lippard, *Anticancer Res.* 34 (2014) 471–476.
- [2] E. Wong, C.M. Giandomenico, *Chem. Rev.* 99 (1999) 2451–2466.
- [3] D. Wang, S.J. Lippard, *Nat. Rev. Drug Discov.* 4 (2005) 307–320.
- [4] L. Kelland, *Nat. Rev. Cancer* 7 (2007) 573–584.
- [5] S.P. Fricker, *Dalton Trans.* (2007) 4903–4917.
- [6] N.J. Wheate, S. Walker, G.E. Craig, R. Oun, *Dalton Trans.* 39 (2010) 8113–8127.
- [7] N.P. Farrell, *Curr. Top. Med. Chem.* 11 (2011) 2623–2631.
- [8] D.J. Stewart, *Crit. Rev. Oncol. Hematol.* 63 (2007) 12–31.
- [9] C.A. Rabik, M.E. Dolan, *Cancer Treat. Rev.* 33 (2007) 9–23.
- [10] R.B. Weiss, M.C. Christian, *Drugs* 46 (1993) 360–377.
- [11] S.J.L.P. Pill, J.R. Bertino, *Vol. 1*, Academic Press, San Diego, 1997.
- [12] J.T. Hartmann, H.P. Lipp, *Expert. Opin. Pharmacother.* 4 (2003) 889–901.
- [13] A.S. Abu-Surrah, M. Kettunen, *Curr. Med. Chem.* 13 (2006) 1337–1357.
- [14] R.C. Todd, S.J. Lippard, *Metallomics* 1 (2009) 280–291.
- [15] A.V. Klein, T.W. Hambley, *Chem. Rev.* 109 (2009) 4911–4920.
- [16] R.P. Perez, *Eur. J. Cancer* 34 (1998) 1535–1542.
- [17] U. Jungwirth, C.R. Kowol, B.K. Keppler, C.G. Hartinger, W. Berger, P. Heffeter, *Antioxid. Redox Signal.* 15 (2011) 1085–1127.
- [18] H. Barry, C.M. Veronique, L.L. Hua, *FEBS Lett.* 486 (2000) 10–13.
- [19] S. Sultana, K. Verma, R. Khan, *J. Pharm. Pharmacol.* 64 (2012) 872–881.
- [20] M. Kruidering, B. Van de Water, E. de Heer, G.J. Mulder, J.F. Nagelkerke, *J. Pharm. Pharmacol. Exp. Ther.* 280 (1997) 638–649.
- [21] Y.I. Chirino, J. Pedraza-Chaverri, *Exp. Toxicol. Pathol.* 61 (2009) 223–242.
- [22] A. Laurent, C. Nicco, C. Chereau, C. Gouvestre, J. Alexandre, A. Alves, E. Levy, F. Goldwasser, Y. Panis, O. Soubrane, B. Weill, F. Batteux, *Cancer Res.* 65 (2005) 948–956.
- [23] H. Masuda, T. Tanaka, U. Takahama, *Biochem. Biophys. Res. Commun.* 203 (1994) 1175–1180.
- [24] A. Sodhi, P. Gupta, *Int. J. Immunopharmacol.* 8 (1986) 709–714.
- [25] A.-B. Witte, K. Anestål, E. Jerremalm, H. Ehrsson, E.S.J. Arnér, *Free Radic. Biol. Med.* 39 (2005) 696–703.
- [26] I. Judson, L.R. Kelland, *Drugs* 59 (2000) 29–36.
- [27] M.R. McLemore, *Clin. J. Oncol. Nurs.* 10 (2006) 559–560.
- [28] S.J. Shi, H.L. Sings, J.T. Bryan, B. Wang, Y. Wang, H. Mach, M. Kosinski, M. W. Sitrin, M.W. Washabaugh, E. Barr, *Clin. Pharmacol. Ther.* 81 (2007) 259–264.
- [29] M.J. Cleare, J.D. Hoeschele, *Bioinorg. Chem.* 2 (1973) 187–210.
- [30] T.W. Hambley, *Chem. Aust.* 58 (1991) 154–156.
- [31] K.S. Lovejoy, S.J. Lippard, *Dalton Trans.* (2009) 10651–10659.
- [32] N. Farrell, *Met. Ions Biol. Syst.* 42 (2004) 251.
- [33] N.J. Wheate, J.G. Collins, *Curr. Med. Chem. : Anti-Cancer Agents* 5 (2005) 267–279.
- [34] N.J. Wheate, J.G. Collins, *Coord. Chem. Rev.* 241 (2003) 133–145.
- [35] L.K. Webster, G.B. Deacon, D.P. Buxton, B.L. Hillcoat, A.M. James, I.A.G. Roos, R. J. Thomson, L.P.G. Wakelin, T.L. Williams, *J. Med. Chem.* 35 (1992) 3349–3353.
- [36] T. Talarico, D.R. Phillips, G.B. Deacon, S. Rainone, L.K. Webster, *Investig. New Drugs* 17 (1999) 1–15.
- [37] J. Czaplá-Masztafiak, J. Nogueira, E. Lipiec, W.M. Kwiatek, B.R. Wood, G. B. Deacon, Y. Kayser, D.L.A. Fernandes, M.V. Pavliuk, J. Szlachetko, L. Gonzalez, J. Sa, *J. Phys. Chem. Lett.* 8 (2017) 805–811.
- [38] R. Haputhanthri, R. Ojha, E.I. Izgorodina, S.-X. Guo, G.B. Deacon, D. McNaughton, B.R. Wood, *Vib. Spectrosc.* 92 (2017) 82–95.
- [39] E. Lipiec, F.S. Ruggeri, C. Benadiba, A.M. Borkowska, J.D. Kobierski, J. Miszczyk, B.R. Wood, G.B. Deacon, A. Kulik, G. Dietler, W.M. Kwiatek, *Nucleic Acids Res.* 47 (2019), e108.
- [40] K. Al-Jorani, A. Rütger, R. Haputhanthri, G.B. Deacon, H.L. Li, C. Cullinane, B. R. Wood, *Analyst* 143 (2018) 6087–6094.
- [41] K. Al-Jorani, A. Rütger, M. Martin, R. Haputhanthri, G.B. Deacon, H.L. Li, B. R. Wood, *Sensors* 18 (2018) 4297.
- [42] C.M. Giandomenico, M.J. Abrams, B.A. Murrer, J.F. Vollano, M.I. Rheinheimer, S. B. Wyer, G.E. Bossard, J.D. Higgins, *Inorg. Chem.* 34 (1995) 1015–1021.
- [43] M. Ravera, E. Gabano, I. Zanellato, F. Fregonese, G. Pelosi, J.A. Platts, D. Osella, *Dalton Trans.* 45 (2016) 5300–5309.
- [44] S.X. Guo, D.N. Mason, S.A. Turland, E.T. Lawrenz, L.C. Kelly, G.D. Fallon, B. M. Gatehouse, A.M. Bond, G.B. Deacon, A.R. Battle, T.W. Hambley, S. Rainone, L. K. Webster, *C. Inorg. Biochem.* 115 (2012) 226–239.
- [45] E.T. Lawrenz, *PhD thesis*, Monash University, 1996.
- [46] R.A. Taylor, D.J. Law, G.J. Sunley, A.J.P. White, G.J.P. Britovsek, *Chem. Commun.* 2008, pp. 2800–2802.
- [47] S. Shamsuddin, C.C. Santillan, J.L. Stark, K.H. Whitmire, Z.H. Siddik, A. R. Khokhar, *J. Inorg. Biochem.* 71 (1998) 29–35.
- [48] Y.-A. Lee, K. Ho Yoo, O.-S. Jung, *Inorg. Chem. Commun.* 6 (2003) 249–251.
- [49] G. Canil, S. Braccini, T. Marzo, L. Marchetti, A. Pratesi, T. Biver, T. Funaioli, F. Chiellini, J.D. Hoeschele, C. Gabbiani, *Dalton Trans.* 48 (2010) 10933–10944.
- [50] J. Abrams Michael, M. Giandomenico Christen, A. Murrer Barry, F. Vollano Jean, Johnson Matthey Inc, US19910723971, 1991.
- [51] I. Romero-Canelon, P.J. Sadler, *Inorg. Chem.* 52 (2013) 12276–12291.
- [52] U. Jungwirth, C.R. Kowol, B.K. Keppler, C.G. Hartinger, W. Berger, P. Heffeter, *Antioxid. Redox Signal.* 15, 2011, pp. 1085–1127.
- [53] R. Ojha, A. Nafady, M.J.A. Shiddiky, D. Mason, J.F. Boas, A.A.J. Torriero, A. M. Bond, G.B. Deacon, P.C. Junk, *ChemElectroChem* 2 (2015) 1048–1061.
- [54] R. Ojha, J.F. Boas, G.B. Deacon, P.C. Junk, A.M. Bond, *J. Inorg. Biochem.* 162 (2016) 194–200.
- [55] G.B. Deacon, B.M. Gatehouse, J. Ireland, *Aust. J. Chem.* 44 (1991) 1669–1681.
- [56] P.S. Braterman, *Reactions of Coordinated Ligands vol. 1*, Plenum Press, New York, Springer US, 1986.
- [57] E. Wissing, J.T.B.H. Jastrzebski, J. Boersma, G. van Koten, *J. Organomet. Chem.* 459 (1993) 11–16.
- [58] G.V. Koten, K. Vrieze, in: F.G.A. Stone, R. West (Eds.), *Advances in Organometallic Chemistry Vol. 21*, Academic Press, 1982, pp. 151–239.
- [59] R. Campbell, P. García-Álvarez, A.R. Kennedy, R.E. Mulvey, *Chem. Eur. J.* 16 (2010) 9964–9968.
- [60] M. Veith, B. Schillo, V. Huch, *Angew. Chem. Int. Ed.* 38 (1999) 182–184.
- [61] M. Veith, A. Rammo, *Z. Anorg. Allg. Chem.* 623 (1997) 861–872.
- [62] L. Pauling, *The Nature of the Chemical Bond*, 2nd ed., Cornell University Press, New York, 1940.
- [63] A.G. Orpen, L. Brammer, F.H. Allen, O. Kennard, D.G. Watson, R. Taylor, *J. Chem. Soc. Dalton Trans.* (1989) S1–S83.
- [64] S.C. Nyburg, C.H. Faerman, *Acta Cryst B41* (1985) 274–279.
- [65] T.W. Hambley, *Inorg. Chem.* 37 (1998) 3767–3774.
- [66] R. Ojha, P.C. Junk, G.B. Deacon, A.M. Bond, *Supramol. Chem.* 30 (2018) 418–424.
- [67] M.H. Chisholm, H.C. Clarck, L.E. Manzer, *J. Am. Chem. Soc.* 94 (1972) 5087–5089.
- [68] T.G. Appleton, H.C. Clarck, L.E. Manzer, *Coord. Chem. Rev.* 10 (1973) 335–422.
- [69] A.R. Battle, A.M. Bond, A. Chow, D.P. Daniels, G.B. Deacon, T.W. Hambley, P. C. Junk, D.N. Mason, J. Wang, *J. Fluor. Chem.* 131 (2010) 1229–1236.

- [70] T.M. McPhillips, S.E. McPhillips, H.J. Chiu, A.E. Cohen, A.M. Deacon, P.J. Ellis, E. Garman, A. Gonzalez, N.K. Sauter, R.P. Phizackerley, S.M. Soltis, P. Kuhn, *J. Synchrotron Radiat.* 9 (2002) 401–406.
- [71] in *(Bruker AXS: Madison, WI)*, Apex2 v 2.0 ed, 2005.
- [72] W. Kabsch, *J. Appl. Crystallogr.* 26 (1993) 795–800.
- [73] G.M. Sheldrick, *Acta Crystallogr. Sect. A* 64 (2008) 112–122.
- [74] G. Sheldrick, *Acta Crystallogr. Sect. C* 71 (2015) 3–8.
- [75] L.J. Barbour, *J. Supramol. Chem.* 1 (2001) 189–191.
- [76] J.C. Oxley, J. Brady, S.A. Wilson, J.L. Smith, *J. Chem. Health Saf.* 19 (2012) 27–33.
- [77] C. Schmidt, L. Albrecht, S. Balasubramanian, R. Misgeld, B. Karge, M. Brönstrup, A. Prokop, K. Baumann, S. Reichl, I. Ott, *Metalomics* 11 (2019) 533–545.
- [78] N.P. Cowieson, D. Aragao, M. Clift, D.J. Ericsson, C. Gee, S.J. Harrop, N. Mudie, S. Panjikar, J.R. Price, A. Riboldi-Tunnicliffe, R. Williamson, T. Caradoc-Davies, *J. Synchrotron Radiat.* 22 (2015) 187–190.